"Sapienza" Università degli studi di Roma

QoS-Constrained Traffic Engineering for Interference-affected Wireless Mesh Networks with Network Coding

Dissertation submitted to the Dept. of Information, Electronics and Telecommunication engineering for the degree of

Doctor of Philosophy

in

Information and Communication Engineering

Candidate:
Valentina Polli

Supervisor:
Prof. Enzo Baccarelli

2012

© Copyright by Valentina Polli, 2012
All Rights Reserved

To my dearly beloved parents,
Adriana and Arcangelo

Abstract

This thesis focuses on the QoS-constrained Traffic Engineering (TE) of Wireless Mesh Networks (WMNs) affected by Multiple Access Interference (MAI). The goal is to develop a tool for the optimization of network/physical resource allocation that enable to design WMNs supporting multicast multimedia sessions with different Quality of Service (QoS) requirements when intra-session Network Coding (NC), besides routing, can be performed at the network nodes.

A wide-applicability integrated framework is proposed, that allows to jointly optimize session utilities, flow control, QoS differentiation, intra-session network coding, Media Access Control (MAC) design and power control. To cope with the *nonconvex* nature of the resulting cross-layer optimization problem, this thesis proposes a two-level decomposition that provides the means to attain the optimal solution through suitably designed *convex* subproblems. Sufficient conditions for the feasibility of the primary (nonconvex) problem and for the *equivalence* to its related (convex) version are derived. Furthermore, a general procedure to devise simple polyhedral outer-bounds of the capacity region, which will be shown to have a key role in the decomposition, has been developed.

Algorithmic implementation of the two-level decomposition is discussed in both centralized and distributed approaches. Moreover, the asynchronous, iterative Distributed Resource Allocation Algorithm (DRAA), that quickly self-adapts to network time-evolutions (e.g., node failures and/or fading fluctuations), is developed. Numerical results that delve into the potential of both the proposed solution and the resource allocation algorithm, are provided. In detail, the two-level decomposition will be tested in unicast, multicast and multisource scenarios so as to show the performance gain achievable by the joint optimization with respect to the conventional solutions.

Contents

List of Figures

List of Tables

List of Acronyms

AP	Access Point
AODV	Ad-hoc On-demand Distance Vector
AP	Access Point
ATM	Asynchronous Transfer Mode
BER	Bit Error Rate
CBR	Constraint Based Routing
CDMA	Code Division Multiple Access
DiffServ	Differentiated Services
DLLSC	Distributed LossLess Source Coding
DM-PIM	Dense Mode-Protocol Independent Multicast
DRAA	Distributed Resource Allocation Algorithm
DSDV	Destination-Sequenced Distance-Vector
DSR	Dynamic Source Routing
ECMP	Equal Cost MultiPath
ERAP	Efficient Resource Allocation Problem
FDMA	Frequency Division Multiple Access
FGS	Fine Granularity Scalable
FNCP	Flow Network Coding Problem

GP	Geometric Program
GSM	Global System for Mobile communications
IGP	Interior Gateway Protocol
IntServ	Integrated Services
IP	Internet Protocol
ISO	International Organization for Standardization
IU	Information Unit
KKT	Karush-Kuhn-Tucker
LDPC	Low Density Parity Check
LP	Linear Programming
LSP	Label Switched Path
MAC	Medium Access Control
MAI	Multiple Access Interference
MD	Multiple Description
MIP	Mixed Integer Program
MPEG	Moving Picture Experts Group
MPLS	Multi-Protocol Label Switching
MPOP	Multicast Primary Optimization Problem
NECMP	Non-equal traffic distribution among Equal Cost MultiPath
NC	Network Coding
NP	Nondeterministic Polynomial time
OLSR	Optimized Link State Routing Protocol
OSI	Open Systems Interconnection model
QAM	Quadrature Amplitude Modulation
QoS	Quality of Service
RSVP	Resource Reservation Protocol
SC	Source Coding

SINR	Signal to Interference plus Noise Ratio
SPF	Shortest-Path First
SVD	Singular Value Decomposition
SW	Slepian-Wolf
TDMA	Time Division Multiple Access
TE	Traffic Engineering
WiFi	Wireless Fidelty
WLAN	Wireless Local Area Network
WMAN	Wireless Metropolitan Area Network
WiMax	Worldwide Interoperability for Microwave Access
WMN	Wireless Mesh Network
WPAN	Wireless Personal Area Network

Chapter 1

Introduction

The growing popularity of multimedia real-time Internet applications and the widespread usage of wireless devices have underlined the need to consider the Quality of Service (QoS) provisioning an essential attribute of the next-generation wireless networks. However, enabling end-to-end QoS over the Internet has already proven challenging in the wired domain because of the complexity introduced in the network architecture. It becomes even more complex when facing an environment of variable connectivity, interference and scarcity of resources as the one offered by the wireless medium, so that, managing the network effectively and efficiently is proving fundamental.

Traffic Engineering (TE) aims to facilitate efficient and reliable network operations while simultaneously optimizing resource utilization and traffic performance. As it turns out, this is indispensable to provide QoS, as it offers the means for network optimization and bandwidth provisioning. Moreover, in the current process towards wireless ubiquitous connectivity, it is crucial to embed TE and QoS in the special scenario offered by Wireless Mesh Networks (WMNs), which are envisioned to further enhance the capabilities of existing wireless networks.

This chapter will focus on the three principal aspects of this thesis: the QoS concept and the architectures developed to support it, the current TE approaches and WMNs. This is meant to depict the context in which this thesis finds ultimate applicability.

1.1 QoS concept and architectures

Originally developed to support "best-effort" services (like e-mail, web browsing, file transfers and so on), the current Internet architecture has to be enhanced in order to provide the guarantees needed by emerging multimedia applications. Although QoS is a concept hard to capture into a single definition due to the high heterogeneity of user perception and application requirements, it is commonly measured by the following performance parameters (Table 1.1 shows typical QoS requirements for Internet applications as reported in [1]):

- throughput;
- delay and delay-jitter;
- packet-loss ratio.

Taking into account such measures means to develop new communication architectures and to add functionalities to the network elements. Specifically, the efforts in the QoS provisioning over IP have led to the development of two different solutions: the Integrated Services (IntServ) [2] and the Differentiated Services (DiffServ) [3] architectures. The IntServ architecture provides per-flow service guarantees which, even if allow for a better utilization of the network resources, can be deployed only in access networks where the number of flows is limited. On the contrary, the DiffServ approach, which was devised to overcome the implementative complexity of IntServ, proposes a quality differentiation based on service classes and can be applied to large networks.

Service	**QoS**			
	bandwidth (b/s)	delay (ms)	jitter (ms)	loss
Web Browsing	<30.5k	<400	N/A	0
Email	<10k	Low	N/A	0
Audio Broadcasting	60-80k	<150	<100	<0.1%
Video Broadcasting	(MPEG-1) 1.2-1.5M (MPEG-2) 4-60M	<150	<100 <50	<0.001% <0.0001%
Audio Conferencing	(G.711) 80k (GSM) 18k	<100	<400	<1%
Video Conferencing	(H.323) 80k	<100	<400	< 0.01%

Table 1.1: *Typical QoS requirements for Internet applications.*

Scalability has been the key to success of the DiffServ architecture over IntServ: burdensome functionalities, such as traffic classification and conditioning, are confined to border routers; no reservation state is needed in the intermediate nodes; and the per-aggregates management of the QoS allows for interior nodes mainly concerned with simple forwarding. However, to benefit from the positive aspects of each, the mentioned QoS architectures are presently considered as complementary, rather than alternative, technologies to deploy QoS on the Internet (e.g., using IntServ in the access networks and DiffServ in the core) [4].

Whether the QoS provisioning is considered with a flow or class granularity, its actual implementation still requires some sort of connection-oriented Internet adaptation. In the IntServ domain this is achieved by means of the Resource Reservation Protocol (RSVP), which is a Transport Layer protocol designed to provide receiver-initiated resource reservations for data flows. The distinctive

features of the DiffServ architecture make it particularly fit to be implemented on Multi-Protocol Label Switching (MPLS), a reliable 2.5-layer platform upon which the Internet is envisaged to enable QoS services [5]. Natively designed to be complimentary with IP, MPLS offers a series of advantages with respect to the currently employed overlay solutions (ATM, frame-relay) as, for example, minor required overhead and variable-length frames compliance.

1.2 Traffic engineering

One of the common aspects of the presented solutions for the QoS support is that, eventually, they require some form of traffic control. To the natural need for explicit routing solutions, which arises when facing QoS demands, network providers/administrators are likely to add the need for the design of traffic distributions optimizing the available resources. Traffic Engineering (TE) [6] is intended to provide answers to both. In addition to QoS-constrained routing, in fact, goal of TE is the optimization of the global performance of the network.

1.2.1 MPLS-TE vs IP-TE

Initial application of TE principles took place in MPLS-based environments [7]. Through the dedicated Label Switched Paths (LSPs) and the capability of explicit routing, MPLS has been, by nature, envisaged to provide an efficient paradigm for traffic optimization. However, since traffic trunks are delivered through dedicated LSPs, scalability and robustness can become real issues in MPLS-based TE.

Quite different from MPLS-TE is the IP-based TE approach. Common IGPs (Interior Gateway Protocols) have been shown to offer load-balancing and failure resilience capabilities since they automatically compute multiple shortest-paths. Only a slight modification of the basic routing mechanism is re-

	MPLS-TE	IP-TE
Routing mechanism	Explicit, with packet encapsulation	Plain IGP
Routing optimization	Constraint-based routing (CBR)	IGP link weight adjustment
Multipath forwarding	Arbitrary traffic splitting	Even traffic splitting only
Hardware requirement	MPLS capable routers	Conventional IP routers
Route selection flexibility	More flexible (arbitrary path)	Less flexible (shortest path)
Scalability (overhead)	Less scalable	More scalable
Failure impact on traffic delivery	High (backup paths)	Low
Failure impact on TE performance	Low	High

Table 1.2: *MPLS/IP-TE comparison.*

quired in order to distribute traffic over the discovered equal-cost paths. These solutions are commonly referred to as Equal Cost Multipath (ECMP) techniques. As in [8–10], properly adjusting the link weights of a SPF routing can lead to improved network performance. However, although easy to configure and maintain, ECMP solutions bring real advantages only when equal-cost paths exist.

In comparison to the MPLS-based approach, IP-based TE solutions lack flexibility, since explicit routing and uneven traffic splitting are still not supported. Nevertheless, ECMP solutions have better scalability and availability resilience than MPLS-TE, because they require no overhead for dedicated LSPs, and link failures can be coped with without explicit provisioning of backup paths. Table 1.2 [11] summarizes the key differences between MPLS-based and IP-based TE.

Recently, some important novelties have been introduced in the field of IP-TE, by extending the approach originally developed in [10]. Specifically, the main contribution of the work in [10] was to establish that, given set of arbitrary (but not loopy) routes, it is always possible to find a positive link weight configuration such that these routes are, actually, the shortest-paths.

This result has a significant, yet theoretical, consequence since it implies that any globally optimal TE solution can be implemented equivalently by means of Non equal traffic distribution among Equal Cost Multipath (NECMP) as well as with a connection-oriented technique.

The critical issue for the actual application of [10] remains, however, the uneven traffic distribution. One solution to this problem is proposed in [12], where the need for NECMP is overcome by three different heuristic algorithms shown to be capable of achieving near-optimal traffic distribution without changing existing routing protocols nor the forwarding mechanisms. Although the combination of [10] and [12] represents an important step towards concrete effectiveness of IP-TE, still they do not provide QoS guarantees and require centralized control. To solve both these problems, [13] first formulates the TE problem taking into account different (average) minimum bandwidth requirements for each QoS-class, and then develops a set of distributed control laws able to mimic the corresponding connection-oriented solution. However, dealing with QoS provisioning still demand to enable routers with NECMP functionalities, so that in [13] actual implementation of these latter is addressed.

1.2.2 TE for wireless networks

In wired networks, TE proposals have underlined that the overall network performance depends on the interaction of flows, so that, a careful planning of the traffic distribution which takes into account the shared resources (i.e., links and routers) is fundamental for an efficient utilization of these latter. When considering a wireless network, however, flows interfere in much more complex ways and TE approaches for wired networks cannot apply unchanged. The properties of the lower layers, like physical and Medium Access Control (MAC), in fact, have a deep impact on the higher layers: flow control (and routing), in particular, cannot prevent to be dependent on channel variability, lack of in-

frastructure, interference, mobility and power-constrained devices. This unique characteristic of wireless networks results in the fact that routing, in practice, controls the formation, configuration and maintenance of the network topology and, ultimately, the resource deployment. This is the main reason why there is no firm line drawn between routing design and TE in the wireless domain.

The need for a different approach with respect to the wired networks, is reflected in the large variety of routing metrics that have been proposed along with routing protocols. Pursuing minimum delivery delay, load-balancing, and high throughput are only a selection of the goals that have determined the costs of links and paths in the network and have driven the routing decisions.

Many popular wireless network routing protocols, i.e., the proactive Optimized Link State Routing Protocol (OLSR) and Destination Sequenced Distance Vector (DSDV) [14], and the reactive Dynamic Source Routing (DSR) [15] and Ad-hoc On-demand Distance Vector (AODV) [16], are basically minimum hop routing protocols. Although easy to implement, hop-count metrics usually induce to select longer, if less, links so requiring higher transmission powers or experiencing higher packet losses. Both these effects can seriously impair the overall network performance. Other routing metrics and other protocols have been introduced to overcome the inefficiencies of minimum-hop count, some based on link-quality, some on transmission time, etc. (see [17,18]). The main disadvantages of these last, however, are that they impose additional overhead, suffer from inaccuracy and responsiveness to node mobility, and most importantly, cannot really capture the impact of interference. Whereas all these proposals remain relevant, they fail to realize the actual potential of the network resources.

To date, cross-layer design is one of the most promising tools for the performance optimization of wireless networks and, consequently, for TE. It offers the means to simultaneously account for, and control, the different elements

which determine the performance of the entire system. The common ISO/OSI layer model has perfectly matched the features of wired networks, but has been repeatedly proved inadequate for the wireless ones. Cross-layer, on the contrary, widens the possibility of network design well beyond those offered by the layered architecture, through the joint optimization of resource allocation, scheduling and routing (a good survey on cross-layer design can be found in [19]). Such capability is, however, obtained at the expense of an increased system complexity so that current research is directed towards the integration of cross-layer design solutions into wireless communication standards so as to minimize their technological impact while preserving their performance improvements.

1.3 Envisioned application scenario

Wireless Mesh Networks (WMNs) are emerging as a technology for ubiquitous and low-cost connectivity, able to "resolve the limitations and to significantly improve the performance of ad hoc networks, Wireless Local Area Networks (WLANs), Wireless Personal Area Networks (WPANs), and Wireless Metropolitan Area Networks (WMANs)" [20]. In this sense, therefore, they introduce a new paradigm of networking in which different wireless networks take part so as to create a wider communication structure offering interoperability and interconnection capabilities.

The appealing advantages promised by WMNs (reliability, low-cost installation, and so on) come, however, at a greater system complexity. In fact, even if the current technologies (e.g., WiMax and WiFi devices) already allow the deployment of a WMN, how to realize the potential of this new wireless architecture is far from being clearly understood. A brief overview of the concepts of WMNs as well as their applicability is given in the following section.

1.3.1 Wireless mesh networks

The innovative feature of WMNs is that each node operates both as a host and as a router. Forwarding packets of other (neighbouring) nodes besides its own, allows a node to widen the transmission range of the others and, eventually, the whole coverage of the network. This also helps to increase the network reliability since nodes are typically connected to several nodes. WMNs consist of mesh routers, clients and gateways connected in a multihop fashion. Some of the mesh routers are sort of edge routers and provide network access for the clients. Traffic aggregated at the edges is then delivered by the interior routers to the destinations, which can either belong to the mesh network or to other external networks, such as the Internet. Interfaces with these network are provided by the gateway nodes.

Mesh routers, generally nodes with limited mobility, form the WMN backbone and are equipped with multiradio interfaces so as to improve flexibility and connect to different devices. Clients could be stationary, mobile and even form self-organized ad-hoc networks which want to access value-added services through the WMN. They have only a single, generally heterogenous, wireless interface, so that even when supplied with routing capabilities lack bridge/gateway functionalities. Based on the mentioned properties of nodes, WMNs can be classified into three categories:

Infrastructure/backbone: mesh routers interconnect so as to provide an infrastructure for the accessing clients. This type of network enables integration of WMNs with existing wireless networks, through gateway/bridge functionalities of mesh routers;

Client: client nodes form peer-to-peer mesh network among themselves. The client nodes perform routing and configuration as well as providing wireless access to end user applications;

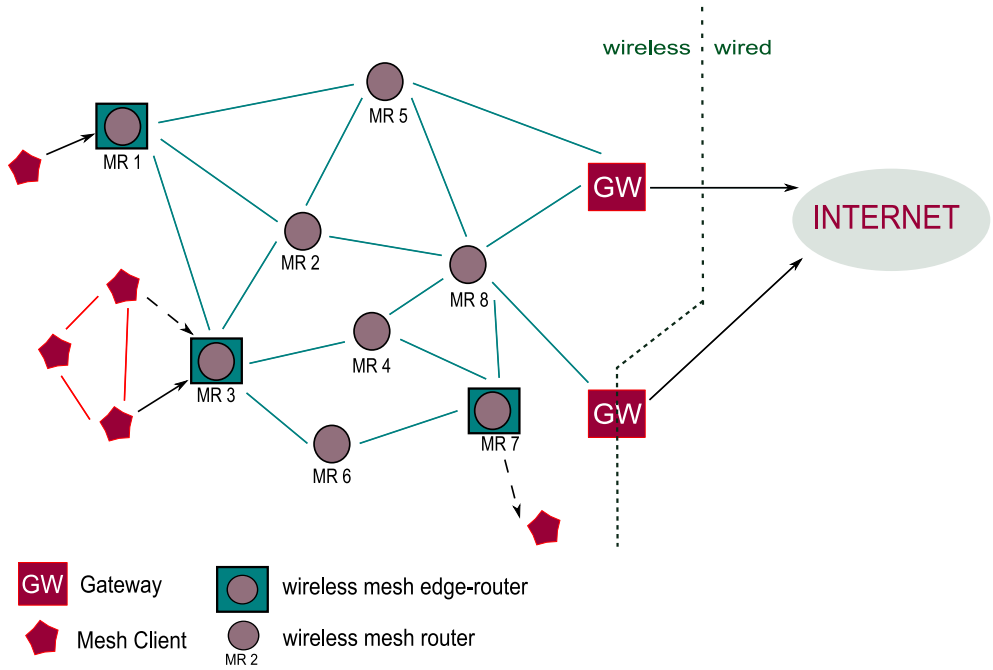

Figure 1.1: *General architecture of WMNs.*

Hybrid: combination of both the above types which, in practice, defines a general reference architecture of WMNs (see Figure 1.1).

The multihop nature of WMNs is the critical factor for both the advantages and the disadvantages of their deployment. On the one hand it allows to enable Internet-based services to the user requiring limited investments on a fixed infrastructure (not all Access Points (APs) need to be wired to the Internet), to widen the coverage area of the network and to improve its reliability. On the other, however, they impose to consider several challenges, such as the ones related to interference and wireless routing, and demand new protocols tailored to their characteristics. Basically, in fact, WMNs are envisioned to

be the wireless counterpart of the Internet, with packets hopping until they reach a given destination, so that they would have to be self-organized and self-configured. This will allow the incremental deployment of the network, in which nodes can join and leave without compromising the network connectivity, and will assure its scalability.

Differently from other ad-hoc networks, WMNs are designed to support broadband services with various QoS requirements. Communication protocols, therefore, have to take into account performance metrics like throughput, end-to-end transmission delay, delay jitter, and packet loss ratios.

Despite the challenges naturally arising from the development of a network with so valuable properties, research on WMNs is motivated by the large number of their possible applications. In fact, they can be employed for:

- last-mile wireless broadband access;
- community and metropolitan networks;
- high-bandwidth in-the-home networking;
- temporary events (concerts, conferences...);
- emergency and public safety applications;
- infrastructure-less scenarios (ships, military...);
- sensor and ad-hoc networks.

Great part of these applications, in fact, cannot be directly supported by cellular, WLANs and other existing wireless networks. As an example, home-networking requires high-bandwidth connections among the separately-located electronic devices. Realizing home-networks with WiFi connections is not convenient for it either demands the careful planning of the AP's location or the

installation of several APs. Mesh networking instead grants a better coverage by means of multihop communications. In community networks, where currently all traffic flows through the Internet, WMNs allows to keep local the share to be delivered within the community. Doing so, bandwidth is saved in the gateways and the needed number of wired APs is reduced. Furthermore WMNs significantly lower the up-front costs in the building of MANs. In fact, they provide higher bandwidth with respect to cellular networks and are far cheaper than the corresponding wired alternatives.

These considerations point out that, due to their distinctive features, WMNs can be employed in numerous applications ranging from simple home and community networks to the "always-on anywhere anytime" connectivity which is critical for emergency applications. Nonetheless, to realize the potential of WMNs considerable research is still needed. MAC and network, as well as application and transport layers have to be suitably modified in order to support the dynamically self-organizing and self-configuring capabilities of WMNs. Moreover, it is a paramount to understand that such innovations should cope with the increasing demands of the consumers for QoS guarantees.

All these aspects contribute to depict the optimal design of a WMN as a really challenging goal and, therefore, make hard to quantify the performance of a particular solution (e.g., routing strategy). This consideration emphasizes the need for a wide-applicability tool that is able to compute the optimal traffic and resource distribution within the WMN that can be used to design the network and as a performance benchmark for the WMNs proposals.

Chapter 2

Related Work and Contributions

Chapter 1 has underlined the need for a clearer understanding of WMNs' potential which can help in developing effective solutions for their actual implementation. QoS provisioning has been shown to be essential for the applications that will have to be supported and TE has proven the key-tool for network design. This chapter surveys previous work in Literature on optimal TE for network-coded WMNs. The goal is to give an appropriate overview of the works related to the topics addressed in this thesis, underline the motivations behind this latter and detail the contributions of this work.

2.1 TE for network-coded WMNs

Traffic engineering for optimal multicast distribution schemes exploiting network coding has been, thus far, investigated mostly for wired networks, where Multiple Access Interference (MAI) is typically negligible and gives rise to *convex* optimization problems [21–25]. Whether the focus is on rate-control (as in [21,23–25]) or on QoS provisioning (as in [22]), having to deal with wired networks means also to deal with *fixed* topologies and *known* link capacities. This, in turn, allows the considered design problems to be shaped in convex,

or even linear, form.

The great potential shown by network coding in terms of both multicast throughput and reliability [26, 27], and recent advantages in its practical implementation [28], have made application of network coding very appealing also in the wireless domain. Network coding can benefit from the broadcast nature of the wireless medium and exploit the so-called "multicast advantage" [29]. In wireless networks, in fact, a single transmission may suffice to simultaneously reach multiple receivers and therefore communications among the network nodes can be arranged so as to minimize the resource consumption of the system. Nevertheless, typical wireless applications must explicitly cope with the side products of using a wireless channel, such as mutual interference and fading phenomena. These factors together with other important aspects of wireless networks (node mobility, failures and power constraints), complicate both the optimal design and the actual implementation of network coding-based multicast schemes, especially when QoS requirements are also to be accounted for.

Initial application of network coding in the wireless domain can be found in [30–32]. The work in [30] aims at finding the minimum-cost multicast scheme for a wireless packet network. In this case, the typical aspects of wireless transmissions, such as power limitations and interference effects are not considered and the feasible rates are simply assumed to belong to a convex set. In [31], the problem of allocating physical and MAC layer resources so as to minimize a network cost-function while meeting desired transmission rates, is considered. To this end, [31] proposes a heuristic procedure to find the minimum-power graphs that are able to support the required capacity and then optimizes to find the sum of max flows assignment in the network layer and the timesharing in the MAC layer. Doing so, the resulting optimization problem becomes convex, but, nonetheless, the algorithm proposed in [31] for selecting the "most

relevant" physical states is *suboptimal* and *centralized*.

In [32], the problem of minimum-energy multicasting, under a layered model of wireless network, is shown to be solved via Linear Programming (LP) when performing network coding. The layered model assumption is based on a decoupling of a, lower, resource-layer and a, upper, network-layer that interact as supply and demand of communication resources. Provided with a set of *realizable* graphs by the resource-layer, the network-layer coordinates flows from sources to destinations so that a required rate is achieved. As in the previous work, the LP formulation of [32] is the result of a timesharing assumption which allows the set of realizable graphs to be comprised of all convex combinations of the elementary graphs. These examples show that, from the very beginning, most published work on network coding for wireless networks has been developed by focusing on cross-layer optimization and has given rise to a variety of solutions whose applicability is often strongly dependent on the assumptions about the MAI. In principle, joint optimization of network resources, such as flows and link capacities, and physical ones (i.e., transmission powers) require to jointly solve: minimum-cost network coding multicasting at the network layer, scheduling at the MAC layer and power control at the physical layer. However, because of the presence of interference, such a problem is generally too complex to be solved, and can only be addressed by means of analytical simplifications/assumptions or by suboptimal/heuristical methods.

In the following, works addressing cross-layer optimization of wireless networks and related topics will be reviewed in accordance with the considered interference scenario.

2.1.1 Interference-free

To date, most cross-layer optimization proposals in Literature have assumed (or reduced to) interference-free operating conditions, either by relying

on the hypothesis of perfect orthogonal access [33–36] or by developing conflict-free schedulers. Time and Frequency Division Multiple Access (T/F-DMA) are shown in [33] to give rise to capacity constraints which are jointly convex in the communication variables in the case of the classical Shannon capacity formula. As a consequence, the simultaneous routing and resource allocation problem addressed in [33] is a convex programming instance and can be solved optimally via dual decomposition. More recently in [34], TDMA is used as a technique to eliminate interference, allowing the link-rate function to be convex in its variables and, therefore, to solve the problem via lagrangian duality.

Timesharing is also the basis of the convexity of the optimization problems considered in [35,36]. As lately formalized in [37], timesharing allows, in fact, to consider link capacities and/or flow rates as belonging to convex resource sets.

Non-interfering communications may be granted also through the design of conflict-free scheduling policies. However, being analogous to graph coloring, such problem has been proved to be NP-hard in [38] for multihop MAI-affected networks, even when the scheduler is centralized [39]. As shown in [40], the same conclusion applies for the FDMA multiuser spectrum allocation. Although, due to the NP-hardness of the problems, all the conflict-free proposals in Literature are suboptimal (see [40–42]), they permit network and physical layers to be designed by means of convex optimization.

2.1.2 Interference-affected

When MAI effects cannot be removed through the implementation of contention avoidance access schemes, cross-layer resource allocation problems are, in general, *nonconvex*. Nevertheless, there have been several attempts to either solve particular instances of the problem or develop manageable *approximations* of the original one.

Since former studies have underlined that the main critical aspect of cross-layer design is represented by the relationship that ties link-capacities to the entire power allocation of the network nodes, a significant research effort has been directed towards finding capacity functions leading to convex problem formulations. Examples can be found in [43–46, 48, 49], where low or high Signal to Interference plus Noise Ratio (SINR) approximations of the Shannon capacity formula have been shown to give rise to convex optimization problems. In detail, [46] proves that, under the high SINR approximation, a variety of power control problems with nonlinear system-wide objectives and QoS requirements can be formulated as Geometric Programs (GPs) and solved by centralized computation through the highly efficient interior point methods [47].

Recently, in [48, 49] the authors have been able to devise a distributed optimal solution for the joint power control, routing/network coding and congestion control problem, for a certain class of capacity functions. Again, the analytical conditions guaranteeing the convexity of the problem can be met only in the high SINR scenario.

Apart from high/low SINR approximation, convexity may arise also from specific constraints/objectives. For example, in [50] log-transformation of the system variables are shown to unveil hidden convexity properties of a particular set of resource allocation problems. Whether convex optimization can be exploited in QoS resource allocation problems for CDMA-based networks with interference has been addressed in [51, 52]. These contributions have proved that necessary and sufficient condition for the convexity of the feasible QoS region is that the SINR can be expressed as a log-convex function of the considered QoS parameters.

Although conveniently solvable by common optimization tools, actual application of the above-cited convex/convexified approaches is limited to the *high SINR* operating scenarios because of the assumptions advanced on the capacity

functions. Low SINRs, in fact, can give rise to *negative* link-capacity values for the capacity functions in [46, 48, 49, 51, 52], so that globally optimal solutions with wide-applicability for the cross-layer design of wireless networks are, to date, an open problem. As pointed out in [46], there are several scenarios that still lead to intractable NP-hard problems whose solution is unknown and that have currently been solved by means of suboptimal and heuristic approaches (see [53] and references therein).

The cited works have been presented in order to give a clear and comprehensive scenario of the strategies devised to manage the nonconvexity due to the presence of interference in cross-layer optimization of wireless networks. Clearly, these works have focused on a different scenario and have each tackled a part of the aspects that will be addressed in this thesis. The closest problem to the one addressed in the following is described in [54]. In detail, [54] tackles the joint optimization of end-to-end transport layer rates, network flows, expected (i.e., long-term averaged) link capacities and power consumption, and instantaneous (i.e., short-term averaged) power allocation policies in MAI-affected faded coded networks with multicast.

Despite the nonconvexity of the resulting optimization problem, [54] proves that dual decomposition is optimal if the network operates under *ergodic* conditions and the gain of each wireless link is a continuous random variable (r.v.). However remarkable, this result arises from the fact that the set of ergodic link capacities generated by all feasible long-term averaged power allocation is convex. This latter condition depicts a scenario which differ from those considered in this thesis in two main aspects. First, the ergodic assumption introduced in [54] cannot apply to the mobility/failure-induced changes in the network connectivity considered here. Second, in agreement with the ergodic assumption, both node powers and link capacities represent expected values, while in this work they are measured on a per-slot basis and represent short-term

averaged values. As a consequence, optimality of dual decomposition cannot be guaranteed. Third, QoS constraints are not taken into account in [54], so that an undifferentiated service model is assumed.

2.1.3 Multisource multicast with network coding

In the last years, the analysis of network coding potentialities have been extended to the case of multisource multicast. In particular, an important result has been proved in [55]. In this work, random linear coding is shown to achieve the multicast capacity asymptotically and, in the context of a distributed source coding problem, also the Slepian-Wolf source-rate region of [56]. This development, supported by the proof of nonoptimality of using separated source and network codes given in [57], has drawn attention to the joint design of distributed source and network encoders for the loss-less transport of data over multi-terminal networks [58–60].

Minimum cost multicasting with lossless source and network coding for wireless networks has been the focus of [61] and [62]. Specifically, [61] developed a distributed rate allocation algorithm which optimizes source and network coding by allowing the sinks to adjust the source rates. Since, in [61], link capacities are fixed and a primary interference model is considered, the addressed problem is stated in convex form, and then solved and distributed by means of its dual. Interference-free communications and fixed capacities are also assumed in [62], where the contra-polymatroid nature of the Slepian-Wolf region is exploited to develop low-complexity greedy-like algorithms capable to attain minimum cost rate and flow allocation. Similarly, a number of MAI-free problems have been examined. Optimal rate and power allocation for the Slepian-Wolf problem is addressed in [60, 63, 64] under the hypothesis of orthogonal access.

2.2 Motivation and main contributions

In conclusion, the presented Literary review has shown that, up to date, optimal cross-layer design of network-coded WMNs has given rise to either limited validity optimal solutions or suboptimal and heuristical ones. These considerations underline the lack of wide-applicability globally optimal QoS-constrained TE strategy for WMNs that can be used as design tool and as a performance benchmark for other solutions.

This provides the motivation to further investigate the possibility to compute the *exact* (i.e., nonapproximate) solution of the MAI-affected *nonconvex* resource allocation problem in which the considered optimal TE reflects, by means of tractable *convex* problems.

To this end, in this thesis, session utilities, flow control, QoS intra-session network coding, MAC design and power control are all embedded into a network-wide cross-layer resource allocation problem, referred to as the Multicast Primary Optimization Problem (MPOP). Furthermore, a multisource generalization of the MPOP is provided, that can take advantage of the potential correlation of the sources when Distributed LossLess Source Coding (DLLSC) is applied jointly with Network Coding. Then, by leveraging on some structural properties of the MPOP, a two-level decomposition of the primary resource allocation problem is developed. This solution combines the performance advantages claimed by the cross-layer approach with the convenience of an optimization-driven decomposition [65], and, most importantly, will be proved to lead to the optimal solution of the nonconvex MPOP.

In detail, main contributions of this thesis may be so summarized:

i) an integrated multi-layer framework for the joint constrained optimization of session utilities and flow control at the Application/Transport layers, QoS intra-session NC at the Network layer, MAI-control at the MAC

layer and power-control at the Physical layer, is developed. The resulting problem constitutes the abovementioned MPOP;

ii) a two-level decomposition of the considered MPOP into two cross-layer interacting sub-problems is carried out, in which the higher-level flow control/NC sub-problem (named Flow Network Coding Problem - FNCP), and the lower-level MAC design/power allocation sub-problem (named Efficient Resource Allocation Problem - ERAP) are *loosely-coupled* (in the sense of [65]). Proper information exchange among these sub-problems is provided by the multicast capacity region $\mathcal{C}$, which may be interpreted as the intersection between the *minimum* set of resources requested by the solution of the FNCP and the *maximum* set of resources available for the solution of the ERAP;

iii) a set of sufficient analytical conditions guaranteeing that, by solving the FNCP on a convex outer bound $\mathcal{C}_0$ of the multicast capacity region, we obtain the *exact* solution of the *nonconvex* MPOP is provided. Furthermore, sufficient conditions for the MPOP feasibility, which rely on a (simple-to-test) set of properties possibly retained by the abovementioned FNCP and ERAP, are derived;

iv) a general procedure for the *closed-form* characterization of tight convex outer bounds $\mathcal{C}_0$'s of any assigned (generally, nonconvex) multicast capacity region $\mathcal{C}$ that *explicitly* account for the MAI effects and approach the actual $\mathcal{C}$ when these last become negligible, is devised;

v) implementation of the two-level decomposition is addressed. Distributed and centralized algorithmic solution are discussed for the two subproblems. The scalable, asynchronous Distributed Resource Allocation Algorithm (DRAA) for the actual implementation of the ERAP that requires

limited exchange of link-state information only among *neighbouring* nodes, is proposed. Such algorithm is proved to *self-adapt* to the occurrence of nonstationary events possibly affecting the network connectivity, as, for example, those due to node-failures and/or fading variations.

On the whole, the presented two-level decomposition can allow to find the optimal QoS-constrained TE solution for WMNs. In practice, this solution can be employed for the optimal design of a WMN and for the performance evaluation of other implementations (e.g., comparison of WMNs' routing metrics).

2.2.1 Thesis organization

The remainder of this thesis is organized as follows. Chapter 3 will describe the multiple multicast MAI-affected power-limited networking scenario, and shows the MPOP formulation. Chapter 4 will focus on the proposed two-level decomposition, its structural properties and detail the outer-bound devising procedure. The implementation analysis of the decomposition and the development of the DRAA are carried out in Chapter 5. Numerical results and performance comparison are provided in Chapter 6, while conclusive remarks are collected in Chapter 7. Important proofs are reported in the final Appendices A and B.

Chapter 3

The Multicast Primary Optimization Problem

This chapter comprises of three parts. The first describes the system model and the assumptions which are the basis of the work. The second is dedicated to the Multicast Primary Optimization Problem (MPOP) and dwells on its constraints and the possible objective functions. Third part proves the wide applicability of the MPOP by showing how its formulation can be easily adjusted to the unicast, multiple unicast and multisource cases.

3.1 System model

The considered wireless mesh network can be represented as a directed graph $\mathcal{G} \equiv (\mathcal{V}, \mathcal{L})$, where $\mathcal{V}$ (with cardinality V) is the set of nodes and $\mathcal{L}$ (with cardinality L) is the set of feasible links (see Figure 3.1). Formally, a directed link l going from the transmit node $t(l)$ to the receive one $r(l)$ is feasible when the gain $g(t(l), r(l))$ of the corresponding physical channel: $t(l) \rightarrow r(l)$ is *strictly* positive. In practice, link l is feasible when the receive node $r(l)$ falls

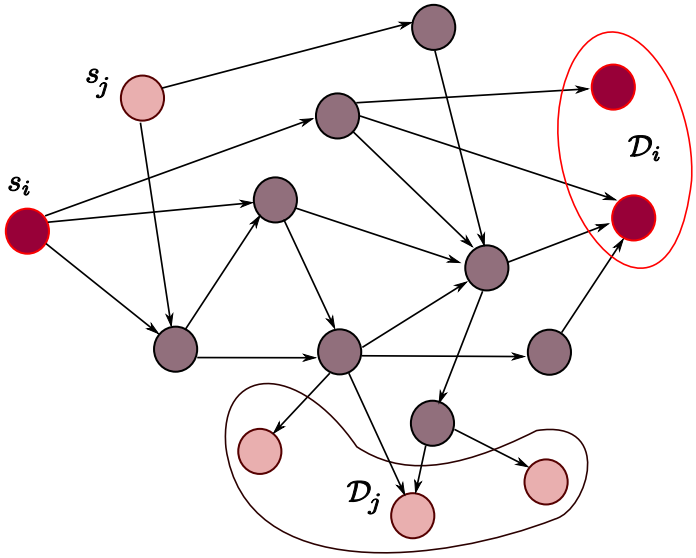

Figure 3.1: *The considered graph model for the wireless network.*

within the transmission range of $t(l)$.

Let $\mathbf{A} \equiv [a(v,l)]$ be the $(V \times L)$ node-link incidence matrix that describes the feasible topology[1] of the network graph $\mathcal{G}$, that is,

$$a(v,l) \triangleq \begin{cases} 1, & \text{if node } v = t(l), \\ -1, & \text{if node } v = r(l), \\ 0, & \text{otherwise,} \end{cases} \tag{3.1}$$

and let $\mathbf{A}_s \equiv [a_s(v,l)] \triangleq \max\{\mathbf{A}, \mathbf{O}_{V\times L}\}$ be the corresponding multicast source matrix. This work relies on a network fluid model [66,67], where $F \geq 1$ rate-elastic multicast sessions, each one identified by the corresponding source/flow/destination-set triplet: $(s_i \in \mathcal{V}, f_i \in \mathbb{R}_0^+, \mathcal{D}_i \subseteq \mathcal{V})$, $i = 1, \ldots F$, distribute

[1] Such matrix *only captures* the feasible network connectivity, whereas the final topology of the network (i.e., the activated links with their relative capacities) is the ultimate outcome of the MPOP.

their traffic flows across multiple paths. $\mathcal{D}_i$ is the destination-set (i.e., the sink-set[2]) of the i-th session, while $\mathcal{D} \triangleq \bigcup_{i=1}^{F} \mathcal{D}_i$ is the overall multicast sink set. Different sessions may share (possibly, multiple) sink nodes, so that the sink-sets $\{\mathcal{D}_i, i = 1, \dots F\}$ may overlap.

To each session-flow f_i (measured in Information Unit per second (IU/s)) corresponds a link-flow vector $\overrightarrow{x_i}$, whose l-th entry, $x_i(l)$, indicates the portion of f_i carried by the l-th link, so that the latter conveys a total flow of

$$x_{_T}(l) \equiv \sum_{i=1}^{F} x_i(l). \tag{3.2}$$

Furthermore, as in [22, 23, 31, 49, 53], intra-session NC is considered as a viable means to improve network efficiency, so that the following relationship holds for $x_i(l)$ [32]:

$$x_i(l) = \max_{j=1,\dots,D_i} \{x_{ij}(l)\}, \tag{3.3}$$

where $x_{ij}(l)$, referred to as the j-th subflow of session i, is the part of $x_i(l)$ intended for the destination $d_j \in \mathcal{D}_i$. Intra-session NC applies to individual multicast sessions, so that the information flows belonging to different sessions are *independently* coded. In general, such coding policy is suboptimal with respect to the more performing inter-session NC, even when the flows of the sessions are mutually independent [26, 68]. However, intra-session NC provides a tractable formal framework for optimization and its actual implementation *does not* require too complex co-decoding operations at both interior and sink nodes [26]. Moreover, intra-session NC typically gives rise to little performance loss (in terms of both conveyed multicast throughput and robustness) with respect to more cumbersome inter-session NC techniques [26, 69].

In agreement with the DiffServ paradigm, each session is assumed to belong to a different service class, which, in turn, demands for specific QoS requirements and priority levels. Hence, without loss of generality, the multicast

[2]The terms sink and destination will be used interchangeably throughout this thesis.

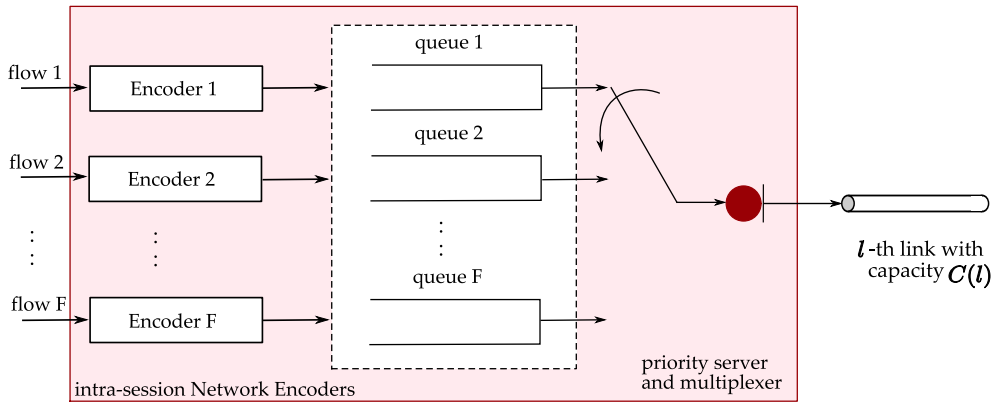

Figure 3.2: *The considered functional model for the l-th output port of interior nodes.*

sessions active over the network are labelled with increasing IDentity numbers (IDs) that correspond to *nonincreasing* priority levels. As a consequence, due to the combined presence of intra-session network coding and multiple service classes, as shown in Figure 3.2, each output port of an interior node is equipped with F intra-session encoders, F parallel queues and a single server, which statistically multiplexes the outgoing flows according to an assigned priority-based service discipline [67].

Since the flow of the i-th session is served at each interior node in accordance with the priority level of the i-th QoS class, the delay function: $\Delta_i(C, x_1, \ldots, x_F)$ adopted to measure the average queue-plus-transmission delay induced by each outgoing link depends on the session-ID i, the overall available link-capacity C, as well as on *all* traffic flows $\{x_1, \ldots, x_F\}$ actually conveyed by the considered link. Hence, as in [67], each per-link session-delay function $\Delta_i(\cdot)$ is assumed:

i) continuous with respect to its $F + 1$ variables;

ii) for any assigned set of variables $\{C, x_1, \dots x_F\}$, nondecreasing in the session-ID i, so that the per-link average delay does not decrease for increasing session-IDs;

iii) for any assigned i and $\{x_1, \dots, x_F\}$, strictly decreasing in C; *iv)* for any assigned i and C, nondecreasing in $\{x_1, \dots, x_F\}$;

iv) for any assigned i, *jointly convex* in the $F+1$ variables $(C, x_1, \dots, x_F)$.

Due to the Kleinrock's independence condition and Jackson's Theorem [67], these (quite mild) assumptions may be reasonably considered met in the considered connectionless networking scenarios, where each end-to-end coded path may be modeled as the cascade of several queueing systems, whose input traffics are the aggregation of multiple flows conveyed by different routes.

Due to the (possible) nomadic behaviour of the considered wireless nodes, each link $l \in \mathcal{L}$ acts as a block-fading channel [70], whose gain may be periodically measured by the corresponding receive node and remains constant over (at least) a slot-time. Besides fading, topological and MAC-related parameters, as well as other network-depending parameters (such as, cross-correlation coefficients of the utilized access codes, beamforming coefficients, etc.) may affect the gain of the physical connection between two nodes. Hence, to capture these last, $\mathbf{G} \triangleq [g(k,l)]$ is defined as the $(L \times L)$ matrix that gathers all the (nonnegative) gains between transmit-receive nodes, i.e.,

$$g(k,l) \triangleq g\left(t(k), r(l)\right), \quad k,l = 1,2, \ \dots L\,.$$

The entries along the main diagonal of $\mathbf{G}$ (i.e., the set of link coefficients $\{g(k,k)\}$) refer to the gains of the feasible links, while the remaining (possibly, nonzero) entries $\{g(k,l),\ k \neq l\}$ are MAI coefficients that measure the interference among different links.

Thus, for each link $l \in L$ with transmit power $P(l)$ (W), the corresponding SINR(l) measured at the receiver node $r(l)$ can be expressed as in [46]

$$\text{SINR}(l) \equiv \frac{\Gamma(l)\, g(l,l)\, P(l)}{\sum\limits_{k=1,\, k\neq l}^{L} g(k,l) P(k) + N(l)}\,, \tag{3.4}$$

where $\Gamma(l) > 0$ is the so-called SINR-gap commonly used to account for the desired target Bit Error Rate (BER) [71], while the denominator in (3.4) is the receiver noise $N(l)$ (W) plus MAI power. The analytical expression of $\Gamma(l)$ in (3.4) depends on the particular codec employed at the l-th link and, as proved in [71], for a M-QAM system is given by

$$\Gamma(l) \approxeq \frac{-1.5\, k(l)}{\log_2(5\, BER(l)^*)} \quad \text{for} \quad BER(l)^* \ll 1/5\,, \tag{3.5}$$

where $BER(l)^*$ is the target BER and $k(l)$ is the coding gain. In the following, $\Gamma(l)$ is only assumed *strictly increasing* in the target BER desired on link l, and, as a consequence, each maximum $BER(l)^*$ value allowed on link l may be equivalently mapped into a corresponding maximum allowed gap-value $\Gamma_{max}(l)$. In this way, the set of gap-constraints:

$$\Gamma(l) \leq \Gamma_{max}(l),\ l = 1, \ldots, L,$$

captures the BER-induced QoS levels to be guaranteed by the Physical layer of the overall network protocol stack.

The resulting capacity $C(l)$ (IU/s) of the l-th link, is *only* assumed to be modeled as a SINR function $\Psi_l(\text{SINR}(l))$, that is *nonnegative*, *continuous* and *strictly increasing* for SINR$(l) \geq 0$, with $\Psi_l(0) \equiv 0$. *Unlike* previous works on the power-control of MAI-affected networks [33, 46, 49, 51, 52], in this thesis, *none* convexity assumption on the behaviour of $C(l)$ is done. The adopted

capacity-function $\Psi_l(\cdot)$ may be link-depending (e.g., due to differences in bandwidth availability at each link). Furthermore, its analytical form is application-depending, and may reflect the statistical behaviour of the fading phenomena impairing the considered link.

All the mentioned per-link parameters may be gathered in the following $(L \times 1)$ column vectors: $\overrightarrow{x_T}$ (total flow vector), $\overrightarrow{x_{ij}}$ (subsession flow vector), $\overrightarrow{\mathrm{SINR}}$ (SINR vector), $\overrightarrow{\Gamma}$ (SINR-gap vector), $\overrightarrow{C}$ (capacity vector) and $\overrightarrow{P}$ (power vector).

3.2 Problem formulation

Let $\overrightarrow{f} \equiv [f_1, \ldots, f_F]$ (IU/s) be the vector collecting the multicast flows generated by all source nodes $\{s_i \in \mathcal{V}\}$. Thus, the goal of the MPOP is to compute the set of network variables $\{\overrightarrow{f}, \overrightarrow{x_1}, \ldots, \overrightarrow{x_F}, \overrightarrow{P}, \overrightarrow{\Gamma}, \mathbf{G}\}$ which minimizes a given network cost-function $\Phi(\cdot)$, while meeting a suitable set of per-session constraints dictated by the Application, Transport, Network, MAC and Physical layers. Specifically, the MPOP is formally stated as follows:

$$\min_{\overrightarrow{f}, \overrightarrow{x_1}, \ldots, \overrightarrow{x_F}, \overrightarrow{P}, \overrightarrow{\Gamma}, \mathbf{G}} \Phi\left(\overrightarrow{f}, \overrightarrow{x_1}, \ \ldots, \overrightarrow{x_F}, \overrightarrow{C}\right), \tag{3.6.1}$$

$$\text{s.t.: } \mathbf{A}\overrightarrow{x_{ij}} - f_i(\overrightarrow{e_{s_i}} - \overrightarrow{e_{d_j}}) = \overrightarrow{0_V}, \ j = 1, \ldots, D_i; \ i = 1, \ldots, F, \tag{3.6.2}$$

$$x_T(l) - \eta(l)C(l) \leq 0, \ l = 1, \ldots, L, \tag{3.6.3}$$

$$\overrightarrow{x_{ij}} - Div(i)f_i \leq \overrightarrow{0_L}, \ j = 1, \ldots, D_i; \ i = 1, \ldots, F, \tag{3.6.4}$$

$$C(l) - C_{max}(l) \leq 0, \ l = 1, \ldots, L, \tag{3.6.5}$$

$$\sum_{l=1}^{L} \varepsilon(l)C(l) - C_{ave} \leq 0, \tag{3.6.6}$$

$$\sum_{l=1}^{L} J_i\left(C(l), x_i(l)\right) - H_t(i) \leq 0, \ i = 1, \ldots, F, \tag{3.6.7}$$

$$B_{min}(i) - f_i \leq 0,\ i = 1, \ldots, F, \tag{3.6.8}$$

$$\sum_{l=1}^{L} \Delta_i \left(C(l), x_{_1}(l), \ldots, x_{_F}(l) \right) - \nabla_t(i) \leq 0,\ i = 1, \ldots, F, \tag{3.6.9}$$

$$\Lambda_i \left(f_i, \sum_{l=1}^{L} \Delta_i(C(l), x_{_1}(l), \ldots, x_{_F}(l)) \right) - \sigma^2_{_D}(i) \leq 0, i = 1, \ldots, F, \tag{3.6.10}$$

$$\overrightarrow{f}, \overrightarrow{x_{ij}} \in \mathbb{R}_0^{+L},\ j = 1, \ldots, D_i,\ \ i = 1, \ldots, F, \tag{3.6.11}$$

$$\Gamma(l) - \Gamma_{max}(l) \leq 0,\ l = 1, \ldots, L, \tag{3.6.12}$$

$$g(l,l) - G_{max}(l) \leq 0,\ l = 1, \ldots, L, \tag{3.6.13}$$

$$-G_{min}(k,l) + g(k,l) \leq 0, l, k = 1, \ldots, L,\ k \neq l, \tag{3.6.14}$$

$$\sum_{l=1}^{L} a_s(v,l) P(l) - P_{max}(v) \leq 0,\ v \notin \mathcal{D}, \tag{3.6.15}$$

$$g(k,l), P(l), \Gamma(l) \geq 0,\ l, k = 1, \ldots, L. \tag{3.6.16}$$

Delving into the reported MPOP constraints, in addition to the usual flow conservation law in (3.6.2) (which, due to the presence of intra-session network coding, applies to each subsession, i.e., to each single source-destination pair), flow vectors $\overrightarrow{x_{ij}}$ and $\overrightarrow{x_{_T}}$ have to comply with the constraints in (3.6.3)-(3.6.4), that upper limit link utilizations. There are several reasons to include such bounds. First, since the f_i's are only *average* measures of the conveyed multicast flows, setting a working condition of $\eta(l) < 1$ may prevent exceeding capacity events arising from traffic-volume fluctuations. Second, the i-th diversity factor $Div(i) \in (0, 1]$ controls the *minimum* number of distinct paths to be employed by the i-th source to each destination $d_j \in \mathcal{D}_i$: specifically, $Div(i) < 1$ guarantees each $d_j \in \mathcal{D}_i$ to be connected by *multiple* different paths to the corresponding source node s_i, so as to provide improved reliability and failure-tolerant properties.

The constraints in (3.6.5)-(3.6.6) may arise from economical restrictions

applied by Network Administrators on the capacity planning of the links [31,66]. These constraints fix a maximum link-capacity $C_{max}(l)$, as well as a maximum average network capacity cost C_{ave}, with a price-rate of $C(l)$ is set to $\varepsilon(l)$. Similarly, the (convex) function $J_i(C(l), x_i(l))$ in (3.6.7) measures the cost to route the flow of the i-th session over the l-th link and may be used to build up suitable session-dependent overlay networks (e.g., Virtual Private Networks) on top of the assigned graph $\mathcal{G}$.

Per-session QoS requirements are forced by (3.6.8)-(3.6.12). Specifically, in addition to the minimum per-session bandwidth $B_{min}(i)$ (IU/s) and maximum per-session delay $\nabla_t(i)$, the maximum average distortion $\sigma_D^2(i)$ tolerated by the sink nodes of the i-th session is accounted for. This bound is media-application specific: as pointed out in [72], each per-session subjective QoS requirement may be measured by a proper convex distortion-function $\Lambda_i(\,\cdot,\,\cdot\,)$ that depends on both i-th bandwidth and delay.

At the MAC Layer, the achievable gains of the feasible network links are *upper limited* by (3.6.13) and the minimum allowed MAI coefficients are *lower limited* by (3.6.14). The former constraint can be used, for example, to bound the maximum transmit antenna gain. The latter describes the interference configuration by means of the G_{min}'s set, which specify the features of the available scheduling strategy (such as, in a CDMA network, the minimum residual cross-correlation term). Therefore, for the considered MPOP, orthogonal access is *feasible* only for vanishing G_{min}'s. A maximum per-link BER is set through the corresponding maximum gap $\Gamma_{max}(l)$ in (3.6.12).

Finally, at the Physical layer, (3.6.15) expresses the maximum power budget per transmit node, while the constraints in (3.6.11), (3.6.16) assure the nonnegativity of all the involved variables.

On the MPOP's objective function

Formally, as in [21,25,53], the objective $\Phi(\cdot)$ function in (3.6.1) is a real-valued, jointly convex function of the link-capacities $\overrightarrow{C}$, session flows $\overrightarrow{f}$ and the link-flows $\overrightarrow{x_i}$, that has to be continuously differentiable up to second order. Since the nondifferentiability of the maximum function in (3.3) affects the differentiability of $\Phi(\cdot)$ (and, likewise, of the some of the MPOP's constraints), in the following (3.3) is replaced with the upper-bound given by the corresponding $\mathcal{L}^n$-norm as in [25,49,73]:

$$x_i(l) \equiv \max_{j=1,\ldots D_i} x_{ij}(l) \leq \Big(\sum_j (x_{ij}(l))^n \Big)^{1/n}. \tag{3.7}$$

This last converges to (3.3) for large[3] n, preserves convexity and guarantee the MPOP to be twice continuously differentiable. The objective function in (3.6.1) may be used to enforce congestion control, network operator goals (e.g., load-balancing and session fairness) or an appropriate trade-off of both. Thus, according to [74], a suitable objective function for the MPOP's framework may assume the following (quite general) form:

$$\Phi(\overrightarrow{f}, \overrightarrow{x_1}, ..., \overrightarrow{x_F}, \overrightarrow{C}) \equiv \theta \left[\sum_{l=1}^{L} \frac{x_T(l)^\beta}{C(l)} \right] - (1-\theta) \left[\sum_{i=1}^{F} U_\alpha(f_i) \right], \tag{3.8}$$

where $\theta \in [0,1]$ is a tunable weight factor, and

$$U_\alpha(f_i) \equiv \begin{cases} \log(f_i), & \alpha = 1 \\ (1-\alpha)^{-1} f_i^{1-\alpha}, & 0 < \alpha < 1 \end{cases} \tag{3.9}$$

is the so-called α-fair utility function adopted to describe the i-th session utility. Load-balancing, whose impact on the objective function increases for increasing values of the exponent $\beta \geq 2$, is enforced by the summation in (3.8) over the link index l.

[3] It has been numerically ascertained that $n = 10$ suffices to guarantee a final accuracy within 1%.

On the per-session delay constraint

In principle, fixing a maximum delay requirement requires to bound the total per-session average delay over each source-destination path. However, since the goal of the MPOP is to find optimal coded routes and link loads, separating the delay contributions arising from different paths joining the same source-destination pair would demand additional *binary* variables per link, which turn the overall MPOP into a Mixed Integer Program (MIP), that is NP-hard to solve. Thus, as in [75], this problem is overcome via the constraint in (3.6.9), that directly bounds the average *total* per-session delay.

On the per-session media distortion function

The i-th distortion function $\Lambda_i : [0, +\infty) \times [0, +\infty) \to [0, +\infty)$ in (3.6.10) describes the average media distortion perceived by each sink-node $d_j \in \mathcal{D}_i$ as a function of both i-th end-to-end multicast flow f_i and corresponding delay:

$$\tau_t(i) \triangleq \sum_{l=1}^{L} \Delta_i(C(l), x_1(l), \ldots, x_{_F}(l)).$$

Formally, $\Lambda_i(\,\cdot\,)$ is assumed nonincreasing for $f_i \geq 0$, nondecreasing for $\tau_t(i) \geq 0$ and jointly convex in $(f_i, \tau_t(i))$. A relevant example of rate-distortion function meeting the above assumptions is the one adopted for describing the performance of Fine Granularity Scalable (FGS) MPEG4-coded video applications in [72]:

$$\Lambda_i(f_i) = \exp\{-a_i f_i + b_i \sqrt{f_i} + c_i\},\ f_i \geq 0, \tag{3.10}$$

with the constants $a_i > 0, b_i \leq 0$ and $c_i \lesseqgtr 0$ tuned in accordance with the statistical features of the actual i-th video sequence. This is, indeed, a relevant example of Multiple Description (MD)-based multimedia coding, where the distortion in (3.10) of the reconstructed video content depends only on the number of IUs (i.e., the number of descriptors) conveyed by the i-th session,

and not specifically on which of them arrive at the intended sink-nodes [76, Chap.17].

3.3 Unicast, multiple unicast and multisource multicast applications

The formulation of the MPOP in (3.6) refers to the *general* case of a multiple multicast networking scenario with intra-session NC and multiple QoS classes. Depending on the number of sources/destinations and sessions actually active over the considered network, the reported MPOP formulation *directly* applies to unicast, multiple unicast and multicast (with/without NC) scenarios. More, it can be easily adapted to the case of multisource sessions with correlated/uncorrelated sources.

3.3.1 Unicast and multiple unicast

Specifically, application of the MPOP to unicast and single-session (coded) multicast is straightforward, since it can be obtained by directly setting: $D_i \equiv F = 1$, and: $F = 1$, respectively. Routing-based multicast and multiple unicast *without* NC may be described by replacing the max-expression in (3.3) with the following summation:

$$x_i(l) = \sum_{j=1}^{D_i} x_{ij}(l)\,, \tag{3.11}$$

that stems from the fact that, in the routing case, each subflow $x_{ij}(l)$ gives rise to an independent uncoded flow (see [32]).

3.3.2 Multisource multicast

The MPOP can also apply to the case of multisource multicast both with correlated and uncorrelated sources. The model presented in Section 3.1 can be

adjusted to the multisource case, simply considering that each multicast session is identified by the corresponding source-set/flow/destination-set triplet: ($\mathcal{S}_i \in \mathcal{V}, f_i \in \mathbb{R}_0^+, \mathcal{D}_i \subseteq \mathcal{V}$), $i = 1, \dots F$. Again $\mathcal{D}_i$ is the destination set, and $\mathcal{S}_i$ is the source sets of the i-th session, while $\mathcal{D} \triangleq \bigcup_{i=1}^{F} \mathcal{D}_i$ and $\mathcal{S} \triangleq \bigcup_{i=1}^{F} \mathcal{S}_i$ are the overall multicast sink and source sets, respectively. Different sessions may share (possibly, multiple) sink and source nodes, so that the sink-sets $\{\mathcal{D}_i, i = 1, \dots F\}$ and the source-sets $\{\mathcal{S}_i, i = 1, \dots F\}$ may overlap.

In order to separate flows belonging to different sources, session flows and flow vectors change as follows. To the s-th source-flow of session i, $f_i(s)$, corresponds a link-flow vector $\overrightarrow{x_i^s}$, whose l-th entry, $x_i^s(l)$, indicates the portion of $f_i(s)$ carried by the l-th link, so that (3.2) becomes

$$x_{_T}(l) = \sum_{i=1}^{F} x_i(l) \equiv \sum_{i=1}^{F} \sum_{s \in S_i} x_i^s(l), \tag{3.12}$$

and the relationship in (3.3) holds for each $x_i^s(l)$, i.e.,

$$x_i^s(l) = \max_{j=1,\dots,D_i} \{x_{ij}^s(l)\}, \tag{3.13}$$

where $x_{ij}^s(l)$, referred to as the j-th subflow of source s of session i, is the part of $x_i^s(l)$ intended for the destination $d_j \in \mathcal{D}_i$. According to this notation, the total session-flow f_i in (3.6) can be expressed as:

$$f_i \equiv \sum_{s \in S_i} f_i(s).$$

Now, let $\{\overrightarrow{f_1}, \dots, \overrightarrow{f_F}\}$ be the $(S \times 1)$ vectors collecting the multicast flows of all source nodes $\{s_i \in \mathcal{S}\}$. Then, the Multisource MPOP (MMPOP) can be defined by the same MPOP formulation in (3.6), provided that:

i) the flow conservation in (3.6.2) is applied to each $\overrightarrow{x_{ij}^s}$ and $f_i(s)$, for all s;

ii) in (3.6.4) $\{x_{ij}(l), f_i\}$ are replaced by $\{x_{ij}^s(l), f_i(s)\}$;

iii) the objective function is rewritten to take into account the different source flows, i.e., it takes the more general form: $\Phi\left(\overrightarrow{f_1}, \ldots, \overrightarrow{f_F}, \overrightarrow{x_1}, ..., \overrightarrow{x_F}, \overrightarrow{C}\right)$;

iv) constraints in (3.6.8) and (3.6.10) are suitably modified in accordance to the source properties.

This last condition implies that in relation to the considered scenario, the maximum distortion and minimum bandwidth requirements can take on different meaning, and form.

Joint source and network coding

Section 2.1.3 has shown how the advantages brought by the application of network coding may be enhanced in the presence of correlated sources. Thanks to the MMPOP formulation defined above, it is possible to model and study also the case of joint source and network coding. Specifically, when LossLess Distributed Source Coding (LLDSC) is performed the maximum distortion and minimum bandwidth constraints of the MMPOP change as follows. First, since sources are assumed to transmit enough information so that their intended sinks are able to exactly recover data by the joint decoding of the flows received from the network, there is no reason to consider a distortion constraint in the MMPOP, and, therefore, (3.6.10) is simply removed. Second, guaranteeing lossless recovery of the source flows means to constrain the set of feasible source rates to the so-called Slepian-Wolf region (see [56]), so that the following expressions

$$H(\mathcal{X}|\mathcal{S}_i \setminus \mathcal{X}) - \sum_{s \in \mathcal{X}} f_i(s) \leq 0, \ \forall \mathcal{X} \subseteq \mathcal{S}_i; \ i = 1, ..., F, \tag{3.14}$$

(where $H(\cdot\,|\,\cdot)$ denotes the conditional entropy operator), take the place of the minimum connection bandwidth requirement in (3.6.8). By means of (3.14), it is possible to take advantage of the potential correlation of the sources and

therefore to reduce the overall load of the network in the presence of correlated streams.

On-the-fly evaluation of the Slepian-Wolf region

The set of conditional entropies $H(\cdot|\cdot)$ at the l.h.s. of (3.14) measures the (spatial) correlation among the source flows to be encoded. Since our paper focuses on the management of the available resources, as in the classic Slepian-Wolf (SW) framework [56], these entropies are assumed known in advance. However, in practical implementations of SW encoders, inter-source correlations need to be estimated and communicated back to the source nodes during the set-up phase of the encoding process, so as to allow the selection of proper codes and coding rates. In wireless scenarios, these correlations can be time-variant and have to be evaluated in real-time, so that rate-adaptive SW coding schemes have to be utilized. In these schemes, each decoder estimates the currently needed coding rate by exploiting the error-detection capability of powerful capacity-achieving Low Density Parity Check (LDPC) codes [77]. A deep discussion of these implementation aspects can be found in [78], where several cases of study are detailed and tested. Finally, it must be pointed out that, after replacing the entropies at the l.h.s. of (3.14) by the corresponding entropy rates, the above MMPOP formulation and its solution still hold if the source flows are jointly ergodic and correlated over both the time and spatial domains.

Chapter 4

The Two-Level Decomposition

The layered approach devised to solve the MPOP defined in Chapter 3 is described here. In detail, this chapter will present the the decomposition level structure, illustrate its fundamental properties and state some feasibility conditions. Furthermore, it will provide significant insights on the capacity regions of nonconvex MPOPs and an effective procedure to design convex outer-bounds.

4.1 The levels definition

Barring the convex bounds in (3.6.7), (3.6.9) and (3.6.10), at first glance, all remaining MPOP's constraints appear linear. Nonetheless, the MPOP is generally *not* a convex optimization problem due to the nonconvexity of the relationship that ties powers and link-capacities (see (3.4)). This implies that, to date, neither guaranteed-convergence iterative algorithms nor closed-form solutions are available to compute the optimal solution $\{\overrightarrow{f}^*, \overrightarrow{x_1}^*, \ldots, \overrightarrow{x_F}^*, \overrightarrow{P}^*, \overrightarrow{\Gamma}^*, \mathbf{G}^*\}$ of the nonconvex MPOP (see [22, 49, 52] and references therein).

A deeper analysis of the MPOP formulation, reveals that link-capacities are not actually part of the set of variables, but introduce, a *loose-coupling* (in the

sense of [65]) between Transport/Network: $\{\overrightarrow{f}, \overrightarrow{x_1}, \ldots, \overrightarrow{x_F}\}$, and MAC/Physical: $\{\overrightarrow{P}, \overrightarrow{\Gamma}, \mathbf{G}\}$ variables. This coupling role can be exploited to devise a two-level solving approach, in which:

- an upper-level tackles the Flow Network Coding Problem (FNCP) in order to compute the optimal link-capacity vector $\overrightarrow{C}^*$;

- a lower-level solves the Efficient Resource Allocation Problem (ERAP), aiming to find the minimum-consumption resource allocation that satisfies the requested link-capacity vector $\overrightarrow{C}^*$.

The presented levels interact by means of the Multicast Capacity Region $\mathcal{C}$ of the MPOP, that is the set comprising all the feasible capacity vectors. To formally define $\mathcal{C}$, let

$$\Pi \triangleq \left\{ \left(\overrightarrow{P}, \overrightarrow{\Gamma}, \mathbf{G} \right) : \text{(3.6.12)-(3.6.16) simultaneously met} \right\}, \tag{4.1}$$

be the convex region of the $(L^2 + 2L)$-dimensional Euclidean space comprising all the triplets $\left(\overrightarrow{P}, \overrightarrow{\Gamma}, \mathbf{G} \right)$ meeting the MAC and Physical layer constraints. Furthermore, let

$$S \triangleq \left\{ \overrightarrow{\text{SINR}} \triangleq [\text{SINR}(1), \ldots, \text{SINR}(L)]^T \right\}, \tag{4.2}$$

be the resulting L-dimensional set of *feasible* SINR vectors, obtained by componentwise application of the scalar relationship in (3.4) to the elements of the set Π in (4.1). Hence, the MPOP capacity region $\mathcal{C}$ can be stated as:

$$\mathcal{C} \triangleq \left\{ \overrightarrow{C} \in \left(\mathbb{R}_0^+ \right)^L : \exists\, \overrightarrow{\text{SINR}} \in S \,:\, C(l) \leq \Psi_l(\text{SINR}(l)),\, l = 1, \ldots, L \right\}. \tag{4.3}$$

On the basis of the definition in (4.3), the FNCP is an optimization problem

in the $\{\overrightarrow{f}, \overrightarrow{x_1}, \ldots, \overrightarrow{x_F}, \overrightarrow{C}\}$ variables, so formulated:

$$\min_{\overrightarrow{f}, \overrightarrow{x_1}, \ldots, \overrightarrow{x_F}, \overrightarrow{C}} \Phi\left(\overrightarrow{f}, \overrightarrow{x_1}, \ldots, \overrightarrow{x_F}, \overrightarrow{C}\right), \tag{4.4.1}$$

$$\text{s.t. : MPOP constraints in (3.6.2)–(3.6.11)}, \tag{4.4.2}$$

$$\overrightarrow{C} \in \mathcal{C}. \tag{4.4.3}$$

Now, let $C^*(l) \in \overrightarrow{C}^*$ indicate the capacity value of link l that is obtained by solving the FNCP in (4.4) and $\text{SINR}^*(l) \triangleq \Psi_l^{-1}(C^*(l))$ the corresponding target SINR. So, the ERAP is defined as

$$\min_{\overrightarrow{P}, \mathbf{G}, \overrightarrow{\Gamma}} \quad \varphi(\overrightarrow{P}, \mathbf{G}), \tag{4.5.1}$$

$$\text{s.t. : MPOP constraints in (3.6.12)–(3.6.16)}, \tag{4.5.2}$$

$$\text{SINR}^*(l)/\text{SINR}(l) - 1 \leq 0, \quad l = 1, \ldots, L, \tag{4.5.3}$$

where the function $\varphi(\overrightarrow{P}, \mathbf{G})$ measures the incurred resource-cost and is introduced to enforce *efficient allocation* of the resources available at the MAC and Physical layers. Since the MPOP objective function $\Phi(\cdot)$ in (3.6.1) depends only implicitly on the power-vector $\overrightarrow{P}$, via the link-capacity vector $\overrightarrow{C}$, it can happen that *multiple* $\overrightarrow{P}^*$'s vectors and $\mathbf{G}^*$'s matrices lead to the *same* optimal capacity vector $\overrightarrow{C}^*$. Hence, task of the objective function in (4.5.1) is to pick up the *most* resource-efficient solution over the set $\{\overrightarrow{P}^*, \mathbf{G}^*\}$ of optimal ones.

As a consequence, the ERAP retains the basic structural property reported in the following proposition.

Proposition 4.1 *When* $\varphi(\overrightarrow{P}, \mathbf{G})$ *in* (4.5.1) *is posynomial in* $\{\overrightarrow{P}, \mathbf{G}\}$, *the* ERAP *becomes an instance of* geometric programming *and, therefore, it is solvable by convex optimization.*

Proof. By definition, a posynomial function $\varphi(z_1, z_2, \ldots, z_n)$ in the nonnegative variables $z_i \geq 0,\ i = 1, \ldots, n$, is the summation [79]: $\sum_{i=1}^{m} g_i(z_1, z_2, \ldots, z_n)$ of

$m \geq 1$ monomial functions: $g_i(\cdot) = c_i \Pi_{j=1}^{n} z_j^{a_{ji}}$, with $c_i > 0$ and $a_{ji} \in \mathbb{R}$, for any $i = 1, \ldots, m$ and $j = 1, \ldots, n$. A Geometric Program (GP) [79] is defined as an optimization problem comprised of posynomial objective and inequality constraints, and monomial equality constraints.

Since the constraint in (4.5.3) is posynomial, and the ones in (4.5.2) are monomial, choosing a posynomial $\varphi(\cdot, \cdot)$ results in a ERAP belonging to the class of GPs. By means of a log-transformation: $y_j \equiv \log z_j$, $j = 1 \ldots n$ of the variables in (4.5.1)-(4.5.3), each monomial can be turned into exponential function with affine-type exponent, and each posynomial into a *log-sum-exp* function. Both exponential and *log-sum-exp* functions are known to be convex so that in this case the ERAP is indeed a convex optimization problem and the claim of Proposition 4.1 directly arises. □

Since the FNCP and the ERAP are loosely coupled problems (in the sense of [65]), their interaction is directly ruled by the optimal capacity vector $\overrightarrow{C}^*$ and the multicast capacity region $\mathcal{C}$. This means that, for the combined FNC-plus-ERA problem, the following formal result holds:

Proposition 4.2 *Let us assume* $\mathcal{C}$ *in* (4.4.3) *be defined as in* (4.3). *Thus, the MPOP in* (3.6) *admits the* same *solution of the combined* FNC-plus-ERA *problem in* (4.4) *and* (4.5).

Proof. From the formal definition of (4.3), it stems out that the multicast capacity region $\mathcal{C}$ *fully* accounts for the overall set of MPOP constraints in (3.6.12)-(3.6.16). This implies that, the FNCP accounts for both the MPOP constraints in (3.6.2)-(3.6.10) via (4.4.2), and the MAC/Physical ones by means of (4.4.3). Hence, the solution $\{\overrightarrow{f}^*, \overrightarrow{x_1}^*, \ldots, \overrightarrow{x_F}^*, \overrightarrow{C}^*\}$ of the FNCP is also the network-solution of the MPOP.

Then, since the ERAP constraints in (4.5.2) are equivalent to the ones in

(3.6.12)-(3.6.16) and the $\overrightarrow{C}^*$-feasibility is taken into account through (4.5.3), the ERAP can be used to find the remaining MAC/Phy-solution of the MPOP, $\{\overrightarrow{P}^*, \mathbf{G}^*, \overrightarrow{\Gamma}^*\}$, and the claim of Proposition 4.2 is proved. □

4.2 Two-level decomposition fundamental property

According to Proposition 4.2, whenever the set of constraints of the ERAP defines a convex multicast capacity region $\mathcal{C}$, both the MPOP and the combined FNC-plus-ERA problem exhibit a convex structure and since their optima coincide the MPOP can be directly solved by means of the two-level decomposition. Unfortunately, this condition is met only for log-convex capacity functions (see [51,52], and the recent contribution in [49]), or when orthogonal access is feasible for the considered MPOP (i.e., when all $\{G_{min}(k,l)\}$ vanish, as in [22]). Nonetheless, the proposed decomposition retains the following key property (proved in the Appendix A), that can allow to compute the *exact* solution of the *nonconvex* MPOP by solving the corresponding *convex* relaxed FNC-plus-ERA problem.

Proposition 4.3 *Let us consider a convex outer-bound $\mathcal{C}_0$ of the multicast capacity region $\mathcal{C}$, i.e., $\{\mathcal{C} \subseteq \mathcal{C}_0\}$, and let $\overrightarrow{C}_0^*$ be the link-capacity vector obtained by solving the $\mathcal{C}_0$-relaxed* FNCP[1]*. Thus, the following properties hold:*

1. *when the $\mathcal{C}_0$-relaxed* FNCP *is unfeasible, then the* MPOP *is unfeasible;*

2. *when the $\mathcal{C}_0$-relaxed* FNCP *is feasible and the* ERAP *is unfeasible (i.e., $\overrightarrow{C}_0^* \notin \mathcal{C}$), then no conclusion may be drawn about the feasibility/unfeasibility of the* MPOP*;*

[1] This problem is still defined by (4.4.1)-(4.4.3), but with $\mathcal{C}$ replaced by the outer-bound $\mathcal{C}_0$.

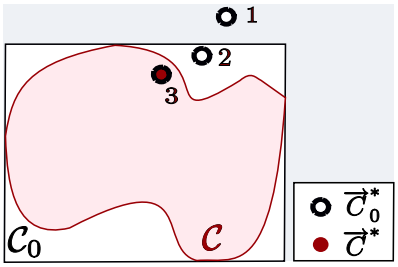

Figure 4.1: *Case study of Proposition 4.3.*

3. *when the* $\mathcal{C}_0$*-relaxed* FNCP *and the* ERAP *are both feasible (i.e.,* $\overrightarrow{C}_0^* \in \mathcal{C}$*), then the* MPOP *is feasible and its link-capacity solution* $\overrightarrow{C}^*$ *coincides with* $\overrightarrow{C}_0^*$. □

An example of capacity region $\mathcal{C}$, convex outer-bound $\mathcal{C}_0$, and corresponding capacity vector solutions of the *FNCP*, $\overrightarrow{C}^*$, and $\mathcal{C}_0$-relaxed *FNCP*, $\overrightarrow{C}_0^*$, are sketched in Figure 4.1, so as to give a pictorial view of the three cases detailed in Proposition 4.3. Specifically, a typical scenario giving rise to Case 1 of Proposition 4.3 occurs when the QoS requirements of the MPOP *cannot* be supported by the available networking resources, so that $\overrightarrow{C}_0^*$ can be represented by a point (marked by 1 in Figure 4.1) that falls *outside* both $\mathcal{C}$ and $\mathcal{C}_0$. This means that, to attempt to turn the MPOP into a feasible problem, either the P_{max} values in (3.6.15) should be increased (as in power-limited applications), or the G_{min} coefficients of (3.6.14) should be lowered (when the network is MAI-limited).

Case 2 of Proposition 4.3 happens when the capacity vector $\overrightarrow{C}_0^*$ belong to the difference set: $\mathcal{C}_0 \setminus \mathcal{C}$ (see point 2 in Figure 4.1). From a practical point of view, in this case, depending on whether the MPOP is feasible or not, it may result that the adopted outer-bound $\mathcal{C}_0$ is too loose to solve the MPOP (see Figure 4.1). Thus, the currently adopted outer-bound $\mathcal{C}_0$ should be replaced

with a tighter one $\mathcal{C}_0'$, in order to (possibly) attain Case 3 of Proposition 4.3. Occurrence of this latter, in fact, guarantees that the computed solution of the corresponding convex relaxed FNC-plus-ERA problem, $\overrightarrow{C}_0^*$, *exactly coincides* with the one of the considered nonconvex MPOP, $\overrightarrow{C}^*$.

4.3 Convex outer-bounds of the capacity region

The properties reported in Proposition 4.3 provide a very useful means to give insight into the solution space of a nonconvex optimization problem which would have otherwise remained completely unknown. Furthermore, they underline the key role played by the adopted convex outer-bound $\mathcal{C}_0$ in the solution capability of the proposed two-level decomposition.

In principle, several convex outer-bounds $\mathcal{C}_0$'s of an (assigned) $\mathcal{C}$ can be devised, the tightest one being the corresponding convex hull [79]. Although tighter outer-bounds generally lead to a higher solution capability of the two-level decomposition, they are also more complex to be analytically characterized and may require the solution of NP-hard optimization problems (as in [31]). Therefore, the main goal in the choice of the set $\mathcal{C}_0$, on which to run the decomposition, is to balance *simplicity* with the occurrence rate of Case 3 of Proposition 4.3. To this end, in the following, an effective procedure to devise polyhedral outer-bounds of the actual capacity region is developed.

4.3.1 Polyhedral outer-bounds of the capacity region

The actual capacity of the l-th link, $C(l)$, according to the assumptions in Section 3.1, is nonincreasing in each $P(j)\,, j \neq l$. This means that each $C(l)$ is upper-bounded by the capacity corresponding to the l-th link when the latter is impaired only by the k-th interferer (i.e., when $P(j) \equiv 0$ for any $j \neq k$ and

$j \neq l$), so that:

$$C(l) \leq \Psi_l \left(G_{max}(l), \Gamma_{max}(l), N(l), G_{min}(k,l), P(l), P(k) \right) \ , k \neq l. \qquad (4.6)$$

By the inversion of (4.6), it is possible to obtain the minimum $P(l)$ needed to support $C(l)$, i.e.,

$$P(l) \geq P_{min}(l) \equiv \Psi_l^{-1} \left(G_{max}(l), \Gamma_{max}(l), N(l), G_{min}(k,l), C(l), P(k) \right). \quad (4.7)$$

On the other hand, for the k-th link, being $\Psi_k(\,\cdot\,)$ nondecreasing in SINR(k), the capacity $C(k)$ is always bounded by

$$C(k) \leq \Psi_k(G_{max}(k), \Gamma_{max}(k), N(k), G_{min}(l,k), P_{max}(t(k)), P(l)). \qquad (4.8)$$

The bound in (4.8) applies also to the case of $P_{min}(l)$ given in (4.7), so that it is possible to derive the maximum feasible $C(k)$ in terms of $C(l)$:

$$C(k) \leq \Psi_k \left(G_{max}(k), \Gamma_{max}(k), N(k), G_{min}(l,k), P_{max}(t(k)), P_{min}(l) \right) \ , \quad (4.9)$$

and, ultimately, express this relationship as follows

$$C(k) \leq \Psi_k \left(\Psi_l^{-1}(C(l)) \right). \qquad (4.10)$$

This bound depends on $C(l)$ as well as on the set $\{G_{min}(l,k), G_{min}(k,l), N(k), N(l), P_{max}(t(k)), G_{max}(k), \Gamma_{max}(k), G_{max}(l), \ \Gamma_{max}(l)\}$ of *fixed local* parameters and accounts for the MAI induced by the links on each other.

Although the convexity in $C(l)$ of (4.10) cannot be guaranteed *a priori*, because it is tied to the particular analytical properties of the involved capacity functions $\Psi_l^{-1}(\,\cdot\,)$ and $\Psi_k(\,\cdot\,)$, it is always possible to devise an upper-bound

$$\overline{\Psi}_{k,l}(C(l)) \geq \Psi_k(\Psi_l^{-1}(C(l))) \qquad (4.11)$$

which is convex in $C(l)$. In fact, both the capacity function properties detailed in Section 3.1 and the power-limited nature of the nodes compel the region in (4.10) to be finite.

The power constraints in (3.6.15) also define the maximum allowed capacities when the MAI is fully absent, i.e.,

$$C_M(j) \triangleq \Psi_j(\Gamma_{max}(j)G_{max}(j)P_{max}(t(j))/N(j)) \,, j = 1, \ldots, L. \tag{4.12}$$

Since every pair $\{k, l\}$ of mutually interfering links have capacities limited by $\{C_M(k), C_M(l)\}$, the assumed convexity of $\overline{\Psi}_{k,l}(\,\cdot\,)$ can be exploited to guarantee that each couple of points $\{(C(l), \overline{\Psi}_{k,l}(C(l))) : C(l) \leq C_M(l), \overline{\Psi}_{k,l}(C(l)) \leq C_M(k)\}$ lies below the line $\widehat{\Psi}_{k,l}(\,\cdot\,)$ defined by:

$$\widehat{\Psi}_{k,l}(\,\cdot\,) \triangleq (C(l) - C_M(l)) \left(\frac{C_M(k) - \overline{\Psi}_{k,l}(C_M(l))}{\overline{\Psi}_{k,l}^{-1}(C_M(k)) - C_M(l)} \right) + \overline{\Psi}_{k,l}(C_M(l)) \,, \tag{4.13}$$

where $\overline{\Psi}_{k,l}(C_M(l))$ and $\overline{\Psi}_{k,l}^{-1}(C_M(k))$ in (4.13) are the values of the function $\overline{\Psi}_{k,l}(x)$ and its inverse, $\overline{\Psi}_{k,l}^{-1}(y)$, in $x \equiv C_M(l)$ and $y \equiv C_M(k)$, respectively.

The polyhedral outer-bound is then given by the intersection of $L(L-1)$ half-spaces of $\mathbb{R}_0^{+L}$ as follows

$$\mathcal{C}_0 \triangleq \bigcap_{k,l=1,k\neq l}^{L} \mathcal{C}_{k,l} \tag{4.14}$$

where each set $\{\mathcal{C}_{k,l},\ k, l = 1 \ldots L, k \neq l\}$ is so defined:

$$\mathcal{C}_{k,l} \triangleq \begin{cases} C(k) \leq C_M(k) \\ C(l) \leq C_M(l) \\ C(k) \leq (C(l) - C_M(l)) \left(\dfrac{C_M(k) - \overline{\Psi}_{k,l}(C_M(l))}{\overline{\Psi}_{k,l}^{-1}(C_M(k)) - C_M(l)} \right) + \overline{\Psi}_{k,l}(C_M(l)) \,. \end{cases} \tag{4.15}$$

The presented procedure for the development of capacity region outer-bounds stems from a single-interferer assumption and reaches general validity by comprising all the interferers through the intersection of the half-spaces

in (4.14). This means that each $\mathcal{C}_{k,l}$ is, in practice, a half-plane. In principle, it is possible to devise a similar procedure considering the presence of two interferers at one time so as to come up with a more refined solution. However, the analytical representation of this solution has proved to be much more complicated and far less practical than the proposed one.

The polyhedral bound given in (4.14) has three appealing properties. First, its formulation is simple, easy to manage and can be described by local fixed parameters. Second, it is able to approach the actual capacity region when all G_{min}'s vanish, since for negligible MAI's effects it shapes a box-type region. Third, in strong MAI environments which result in deeply concave capacity regions, it gives the tightest convex outer-bound of $\mathcal{C}$.

To illustrate the mentioned properties, an example of practical relevance that reports the analytical expression assumed by $\overline{\Psi}_{k,l}(\cdot)$ in the usual case of logarithmic (i.e., Shannon-like) capacity function is given in the following.

4.3.2 Example: The Shannon capacity function

When applied to the logarithmic Shannon capacity function, i.e.,

$$C(k) \equiv \log_2(1 + \mathrm{SINR}(k)), \tag{4.16}$$

the proposed approach for the development of a polyhedral outer-bound gives rise to a $\Psi_k(\Psi_l^{-1}(C(l)))$ (from now on simply denoted as $\Psi_k(C(l))$) so formulated:

$$\begin{aligned} \Psi_k(C(l)) &\triangleq \log_2\left(1 + \frac{\Gamma_{max}(k)\Gamma_{max}(l)G_{max}(k)G_{max}(l)}{G_{min}(l,k)G_{min}(k,l)\left(2^{C(l)}-1\right)(1+\alpha)+\beta}\right) \\ \alpha &\triangleq \frac{N(l)}{P_{max}(t(k))G_{min}(k,l)} \\ \beta &\triangleq \frac{N(k)\Gamma_{max}(k)G_{max}(k)}{P_{max}(t(k))}\,. \end{aligned} \tag{4.17}$$

By simply discarding β in (4.17), whose direct dependence on $N(k)$ makes negligible, a tight upper-bound of Ψ_k can be readily derived and defined as

$$\overline{\Psi}_{k,l}(C(l)) = \log_2\left(1 + \frac{\chi(k,l)}{2^{C(l)} - 1}\right), \tag{4.18}$$

where

$$\chi(k,l) \triangleq \frac{\Gamma_{max}(l)\Gamma_{max}(k)G_{max}(l)G_{max}(k)}{G_{min}(l,k)G_{min}(k,l)\left(1 + \frac{N(l)}{P_{max}(t(k))G_{min}(k,l)}\right)}. \tag{4.19}$$

This bound is convex in $C(l)$ for any $\chi(k,l) \geq 1$.

Figure 4.2 shows both the projection on links k, l of the actual capacity region, which is described by $\Psi_k(C(l))$, and the convex outer-bound in (4.18) for different MAI scenarios. The plots show how closely the selected bound follows the region depicted by the original capacity function, and underline the dependence on the G_{min}'s values.

The capacity region given by $\Psi_k(C(l))$, its upper-bound $\overline{\Psi}_{k,l}(C(l))$ in (4.18) and the set $\mathcal{C}_{k,l}$ defined in (4.15), are reported in Figure 4.3 for the case of $\chi(k,l) = 90.95$, which is representative of an intermediate MAI configuration. The set $\mathcal{C}_{k,l}$ can be seen as the projection on links k, l of the polyhedral upper-bound in (4.14). From the plots in Figures 4.2 and 4.3 is evident that for a deeply MAI-affected scenario, which gives rise to a concave region, the set $\mathcal{C}_{k,l}$ becomes the convex hull of the actual capacity region, and therefore, the tightest convex outer-bound possible. On the contrary, low MAI cases give rise to almost box-type regions, where the capacities are only limited by the power constraints of the nodes. In this case, the polyhedral outer-bound in (4.14) is also box-shaped and approaches the actual capacity region.

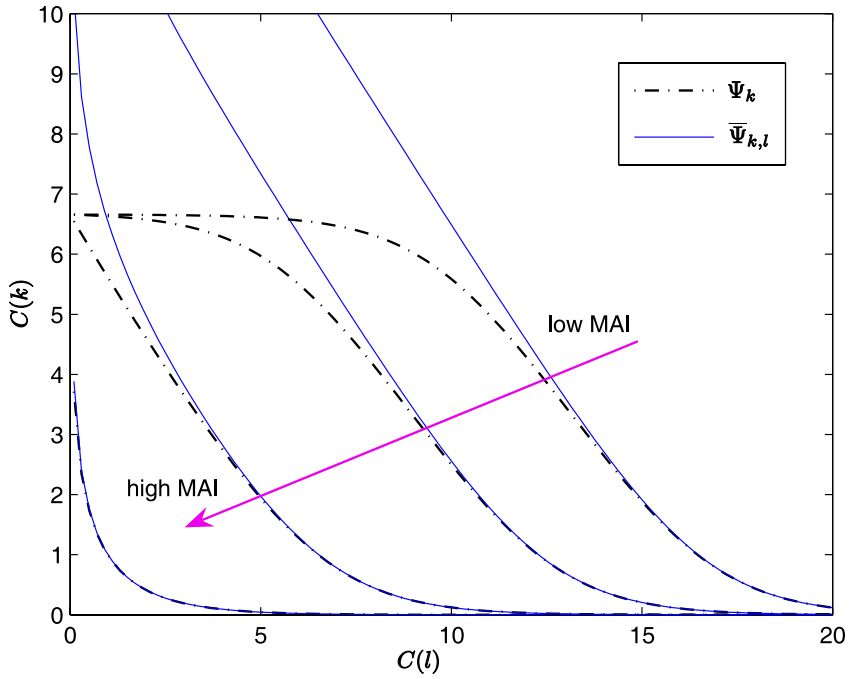

Figure 4.2: *Projection on links k, l of the actual capacity region, $\Psi_k(C(l))$, and convex outer-bound $\overline{\Psi}_{k,l}(C(l))$ for several MAI scenarios.*

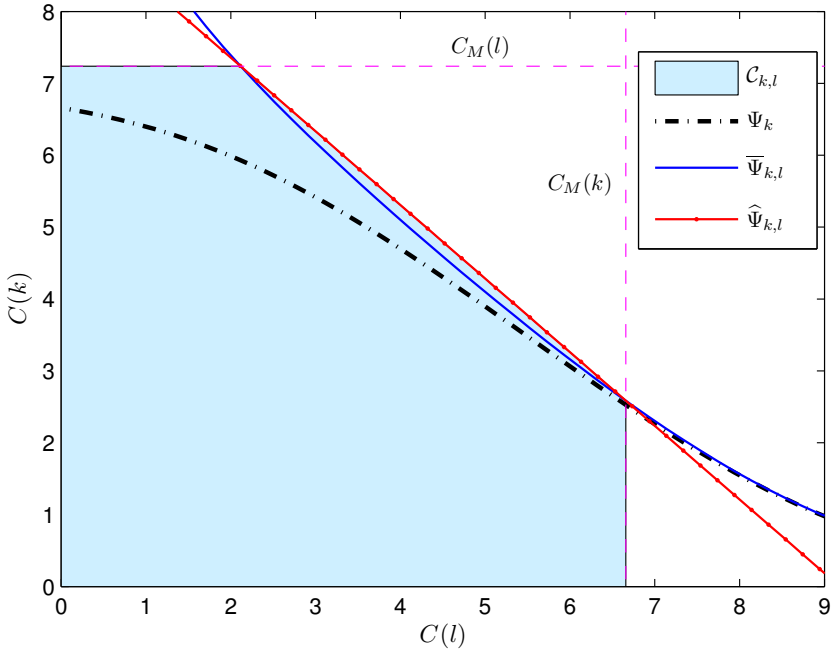

Figure 4.3: *Projection on links k, l of the actual capacity region, defined by $\Psi_k(C(l))$, convex outer-bound $\overline{\Psi}_{k,l}(C(l))$ and corresponding set $\mathcal{C}_{k,l}$.*

4.4 Feasibility of the MPOP

Proposition 4.3 points out that the feasibility of the ERAP suffices for the feasibility of the MPOP and, moreover, for the coincidence of its solution $\overrightarrow{C}^*$ with the one of the FNC-plus-ERA problem, $\overrightarrow{C}_0^*$. As a consequence, the following two conditions (the first necessary and sufficient, the second only sufficient) provided for the feasibility of the ERAP guarantee both the MPOP feasibility and the abovementioned solutions equality: $\overrightarrow{C}^* = \overrightarrow{C}_0^*$.

Proposition 4.4 *Let* $\mathbf{J}$ *be the* $(L \times L)$ *matrix whose* (k,l)*-th entry is*

$$J(k,l) \triangleq \begin{cases} -1, & k = l, \\ \frac{G_{min}(k,l)\Psi_k^{-1}(C_0^*(k))}{G_{max}(k)\Gamma_{max}(k)}, & k \neq l. \end{cases}$$

Thus, if and only if *there exists a* $((V+L)\times 1)$ *nonnegative vector* $\overrightarrow{\beta}$ *that meets the following relationship:*

$$\begin{bmatrix} \mathbf{J} \\ \mathbf{A_s} \end{bmatrix}^T \overrightarrow{\beta} + \overrightarrow{1}_L = \overrightarrow{0}_L, \tag{4.20}$$

the ERAP *is feasible.*

Proof. To guarantee feasibility, the ERAP must allow a solution at least for the following set of *relaxed* link-gain coefficients: $\{g(k,l) \equiv G_{min}(k,l),\ g(l,l) \equiv G_{max}(l),\ \Gamma(l) \equiv \Gamma_{max}(l),\ \forall k \neq l\}$. As far as feasibility is concerned, the ERA problem in (4.5) is equivalent to the following linear program:

$$\min_{\overrightarrow{P}} \{\overrightarrow{1}_L^T \overrightarrow{P}\},\ \text{s.t.} \quad \begin{bmatrix} \mathbf{J} \\ \mathbf{A_s} \end{bmatrix} \overrightarrow{P} \leq \begin{bmatrix} \overrightarrow{d} \\ \overrightarrow{P}_{max} \end{bmatrix}, \tag{4.21}$$

where $d(l) \triangleq \Psi_l^{-1}(C_0^*(l))N(l)/(G_{max}(l)\Gamma_{max}(l))$ is the l-th entry of the vector $\overrightarrow{d}$, and $\overrightarrow{P}_{max}$ is the vector collecting the maximum allowed node powers (see

(3.6.15)). By duality, the problem in (4.21) admits (at least one) solution *if and only if* it is compliant with (4.20) and this proves the sufficient part of the claim. The necessary part stems out from the fact that (4.20) is derived by referring to the *less*-interfered, *highest*-gains and *less* SINR-demanding case. □

A simpler sufficient condition for the feasibility of the considered ERAP may be formulated directly in terms of Singular Value Decomposition (SVD), as reported in the following Proposition 4.5.

Proposition 4.5 *The* ERAP *is feasible* if *the matrix in* (4.20) *allows a non-negative (right) eigenvector* $\overrightarrow{v}$ *that meets the following relationship:*

$$\begin{bmatrix} \mathbf{J} \\ \mathbf{A_s} \end{bmatrix}^T \overrightarrow{v} = \sigma \overrightarrow{u} = -\overrightarrow{1}_L, \tag{4.22}$$

where $\overrightarrow{u}$ *and* σ *are the (left) eigenvector and the singular value of* $\overrightarrow{v}$*, respectively.*

Proof. The sufficient condition in (4.22) can be directly derived from (4.20) by replacing $\overrightarrow{\beta}$ by $\overrightarrow{v}$ and, then, by performing the Singular Value Decomposition (SVD) of the resulting matrix relationship. Since in this case vectors $\overrightarrow{u}$ and $\overrightarrow{v}$ are compelled to be eigenvectors, such condition is only sufficient. □

Chapter 5

Implementation aspects

This chapter is dedicated to the implementation aspects of the proposed decomposition. First, both the Flow Network-Coding Problem and the Efficient Resource Allocation Problem will be analyzed and techniques for their algorithmic solution discussed. Main contribution of the chapter is the development of the Distributed Resource Allocation Algorithm devised to solve the ERAP, and its properties. Then, actual implementation of the proposed algorithmic solutions is investigated.

5.1 The flow network-coding problem

Main task of the FNCP is to compute all the source-destination network-coded routes meeting both the considered per-session sets of QoS requirements and the network constraints. Being comprised by linear/convex constraints and by a convex objective function, the $\mathcal{C}_0$-relaxed FNCP is a convex optimization problem and, provided that the Slater's qualification holds, it can be solved via the common Karush-Kuhn-Tucker (KKT) optimality conditions [79]. These latter, however, give rise to a set of nonlinear equations that ultimately require some kind of Newton-based technique to compute the optimum

$\{\overrightarrow{f}^*, \overrightarrow{x_1}^*, \ldots, \overrightarrow{x_F}^*\}$.

Fortunately, the FNCP can be readily solved by methods like the ones belonging to the interior-point class [47] (e.g., the barrier method) which have, in the last years, proved to be effective means for the solution of convex optimization problems. By combining the high accuracy of the Newton's method with the backtracking linesearch and introducing a logarithmic barrier function, these algorithms are able to show good performance while keeping low the implementative complexity.

Interior point methods may be used either to solve the entire FNCP problem in a centralized way, or applied to its distributed versions, according to the particular application scenario. Both centralized and distributed implementations are further discussed in the next subsection.

5.1.1 Centralized vs. distributed approach

Optimization in the FNCP is performed over local variables: flow vectors $\overrightarrow{x_i}$ and capacities $\overrightarrow{C_i}$ are link-based, and, more, session flows f_i can be obtained by adding up either the outgoing flows at the sources or the incoming ones at the destinations. On the contrary, the set in (4.4.2) consists of end-to-end constraints in addition to the local ones. As it will be shown in the following, this particular feature of the FNCP may prevent the successful application of a primal/dual approach for the development of a distributed solution, which may be viable in other frameworks (see [61]).

In a master/subproblems dual decomposition, end-to-end constraints result in *global* multipliers and in a Lagrangian function which is only partially separable. In the MPOP case, this causes each subproblem to present the following structure

$$\min_{x(l),C(l)} g_l(C(l), x(l), \overrightarrow{b}) \tag{5.1}$$

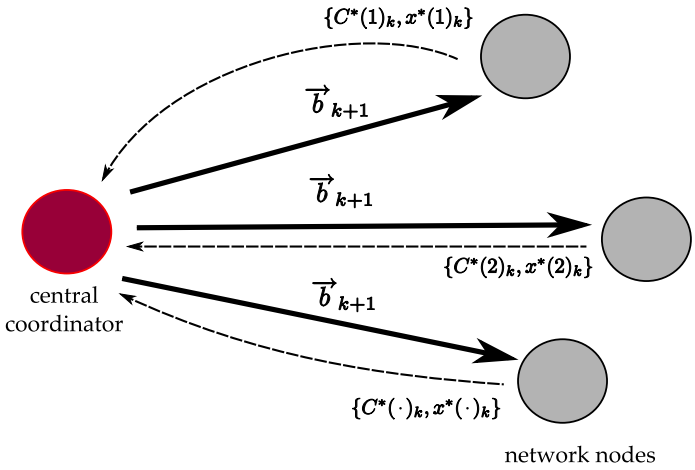

Figure 5.1: *Master/subproblems iterative pricing mechanism.*

s.t.: link-based constraints

and the master problem to be given by

$$\max_{\overrightarrow{b}} \sum_{l} g_l^*(\overrightarrow{b}) + g_b(\overrightarrow{b}) \qquad (5.2)$$
$$\text{s.t.: } \overrightarrow{b} \in \mathbb{R}_0^{+|B|},$$

where vector $\overrightarrow{b}$ collect the $|B|$ global multipliers, $g_b(\cdot)$ and the $g_l(\cdot)$'s are the global and the local parts of the Lagrangian function, and $g_l^*(\overrightarrow{b})$ is the value of $g_l(\cdot)$ calculated in $\{C^*(l), x^*(l)\}$ which is the solution of the problem in (5.1).

This kind of decomposition works according to the "pricing" mechanism depicted in Figure 5.1 [65]. At the k-th step, the master problem floods in the network the "resource price" (i.e., the $\overrightarrow{b}_k$) that is used by the subproblems to compute their best "resource deployment" (i.e., to solve (5.1) and find $\{C^*(l)_k, x^*(l)_k\}$). This information is then fed back to the master and employed in (5.2) to determine the next-iteration prices: $\overrightarrow{b}_{k+1}$. The optimum is reached

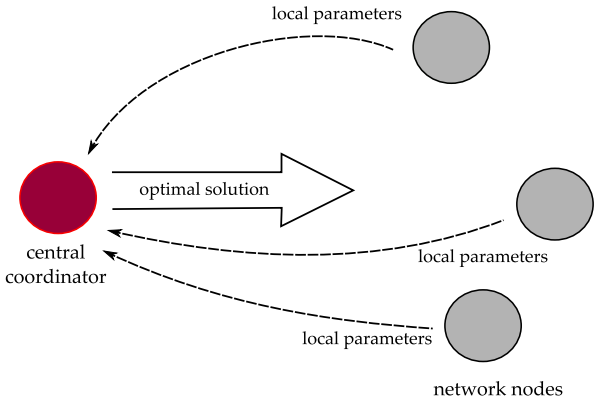

Figure 5.2: *Centralized solution two-step signalling.*

when the master finds the best pricing strategy. This solution, therefore, requires a proper information exchange between the master problem (which is hosted on a central controller) and the subproblems (which run on the network nodes) and, more, that this signalling is iterative and stops only when the optimum is achieved.

Centralized solutions, as shown in Figure 5.2, demand an initial communication from the network nodes to the central coordinator that conveys all the information needed to compute the optimum, and then, the solution flooding from the coordinator to the network. This may imply a significant set-up signalling. However, in most applications, large part of this information (QoS requirements, network operators costs and so on) is naturally owned by source nodes so that choosing them as coordinators means to effectively cut down the actual amount of information exchange.

Clearly, the FNCP is solvable in both ways. Which is the most suitable has to be decided according to the particular instance of the problem at hand and the application involved. Distributed solutions usually require the exchange of

minor quantity of data, but they required it repeatedly (and for large networks, convergence may be obtained after a considerable number of iterations). On the other hand, centralized ones are based on a non-iterative, but wider, signalling. Generally, a good trade-off between quick response and signalling burden may be represented by the choice of a source-driven centralized solution.

5.2 The distributed resource allocation algorithm

As stated in Proposition 4.1, the posynomial structure of the objective function in (4.5.1), allows the ERAP to be recast in a convex form through the following log-transformation of the involved variables: $z_l \triangleq \log(P(l))$, $y_l \triangleq \log(\Gamma(l))$, $\mathbf{W}(k,l) \triangleq [w_{k\,l} \triangleq \log(g(k,l))]$. Although in this case, as in the former, interior point algorithms are still efficient in computing the optimum, the analytical structure of the ERAP can be further exploited to develop a distributed resource allocation algorithm.

To this end, without loss of generality, the objective function of the ERAP is assumed to fall in the class of additively separable functions. The function in (4.5.1), in fact, has been introduced to select the most efficient resource allocation among the optimal ones and does not affect the solution of the primary problem. This means that, in principle, its choice can be completely arbitrary. An effective example of separable objective function that enforces efficient resource allocation is represented by the total network power consumption $\varphi(\overrightarrow{P}, \mathbf{G}) \equiv \sum_{l=1}^{L} P(l)$ which will be adopted in the following discussion and to which every MPOP's instance will refer unless otherwise stated.

With respect to the FNCP, the ERAP comprises of constraints and variables which are both local. This suggests that by pursuing a Lagrangian dual decomposition it is possible to find the optimal resource allocation distribu-

tively. The Lagrangian function associated to (4.5.1)-(4.5.3) is given by:

$$
\begin{aligned}
L(\overrightarrow{z}, \overrightarrow{y}, \mathbf{W}, \overrightarrow{\lambda}) = & \sum_{l=1}^{L} e^{z_l} + \\
& + \sum_{l=1}^{L} \lambda_{1l} \Big(\mathrm{SINR}^*(l)\, e^{-z_l - y_l - w_{ll}} \Big[\sum_{k \neq l}^{L} e^{z_k + w_{kl}} + N(l) \Big] - 1 \Big) + \\
& + \sum_{v=1}^{V-D} \lambda_{2v} \Big(P_{max}(v)^{-1} \sum_{l=1}^{L} a_s(v,l) e^{z_l} - 1 \Big) + \\
& + \sum_{l=1}^{L} \lambda_{3l} \left(e^{y_l} - \Gamma_{max}(l) \right) + \\
& + \sum_{l=1}^{L} \lambda_{4l} \left(e^{w_{ll}} - G_{max}(l) \right) + \\
& + \sum_{l=1}^{L} \sum_{k \neq l}^{L} \lambda_{5kl} \left(e^{-w_{kl}} + G_{min}(k,l) \right) , \qquad (5.3)
\end{aligned}
$$

where $\overrightarrow{\lambda} \triangleq [\overrightarrow{\lambda}_1 \overrightarrow{\lambda}_2 \overrightarrow{\lambda}_3 \overrightarrow{\lambda}_4 \overrightarrow{\lambda}_5]^T$ is the (column) vector collecting all the Lagrangian multipliers corresponding to the constraints in (4.5.2)-(4.5.3).

Since both strong duality and Lagrangian min-max equality hold [79], the optimal solution is represented by the *saddle point*, which is the feasible point satisfying:

$$\nabla L(\overrightarrow{z}^*, \overrightarrow{y}^*, \mathbf{W}^*, \overrightarrow{\lambda}^*) = 0. \qquad (5.4)$$

Solution to (5.4) can be *iteratively* computed on a per-slot basis by means of a gradient-based method, in which the variable u at the $(k+1)$-iteration is obtained as:

$$u^{(k+1)} = u^{(k)} - a_u^{(k)} \nabla_u L \left(\overrightarrow{z}^{(k)}, \overrightarrow{y}^{(k)}, \mathbf{W}^{(k)}, \overrightarrow{\lambda}^{(k)} \right) . \qquad (5.5)$$

According to the results in [80], a stepsize sequence $\{a_u^{(k)}\}$ in (5.5) which sat-

isfies the following:

$$a_u^{(k)} > 0, \tag{5.6}$$
$$\sum_{k=0}^{\infty} a_u^{(k)} = \infty\,,$$
$$\sum_{k=0}^{\infty} (a_u^{(k)})^2 < \infty\,,$$

guarantees the convergence of the iterative algorithm to the optimal solution.

For each link-index $l = 1, \ldots, L$, with $k \neq l$, the gradients in (5.5) are as follows:

$$\nabla_{z_l} L = e^{z_l} + \sum_{k \neq l}^{L} D_k e^{w_{lk}+z_l} + \sum_{v=1}^{V-D} e^{z_l} \lambda_{2v} \frac{a_s(v,l)}{P_{max}(v)} - D_l I_l, \tag{5.7.1}$$

$$\nabla_{y_l} L = -D_l I_l + \lambda_{3l} e^{y_l}, \tag{5.7.2}$$

$$\nabla_{w_{ll}} L = -D_l I_l + \lambda_{4l} e^{w_{ll}}, \tag{5.7.3}$$

$$\nabla_{w_{kl}} L = D_l\, e^{z_k + w_{kl}} - \lambda_{5kl} G_{min}(k,l) e^{-w_{kl}}, \tag{5.7.4}$$

$$\nabla_{\lambda_{1l}} L = \Psi_l^{-1}(C_0^*(l))\, e^{-z_l - y_l - w_{ll}} I_l - 1, \tag{5.7.5}$$

$$\nabla_{\lambda_{2_v}} L = P_{max}(v)^{-1} \sum_{l=1}^{L} a_s(v,l) e^{z_l} - 1, \tag{5.7.6}$$

$$\nabla_{\lambda_{3l}} L = e^{y_l} - \Gamma_{max}(l), \tag{5.7.7}$$

$$\nabla_{\lambda_{4l}} L = e^{w_{ll}} - G_{max}(l), \tag{5.7.8}$$

$$\nabla_{\lambda_{5kl}} L = e^{-w_{kl}} + G_{min}(k,l). \tag{5.7.9}$$

In the above expressions, $\overrightarrow{C}_0^* \triangleq [C_0^*(1), \ldots, C_0^*(L)]^T$ is the link-capacity vector solution of the $\mathcal{C}_0$-relaxed FNCP,

$$I_l \triangleq \sum_{k=1,\, k \neq l}^{L} e^{z_k + w_{kl}} + N(l), \tag{5.8}$$

is the aggregate MAI-plus-noise power-level affecting the l-th link, while

$$D_l \triangleq \lambda_{1l} \Psi_l^{-1}(C_0^*(l))\, e^{-z_l - y_l - w_{ll}}, \tag{5.9}$$

is the (scaled) SINR target value of link l.

Basing on the analysis of the features of (5.3) and (5.7), which confirm that the involved variables and multipliers are *local quantities*, the presented gradient-based solution is named the Distributed Resource Allocation Algorithm (DRAA). According to (5.7), in fact, most of the presented gradients completely relies on local information so that each node is able to autonomously find its own optimal resource allocation simply by means of the set of updates in (5.5)-(5.7) related to its links, provided that it can get the remaining *nonlocal* information. For the l-th link, such information is entirely described by I_l (which depends on the other nodes power) and by the set of D_k's in (5.7.1).

These, in principle, have to be acquired through a proper data exchange among the network nodes at each iteration. However, since I_l may be *measured* directly at the receive node $r(l)$ of link l, D_l in (5.9) is the only information left to be exchanged by the network nodes. Furthermore, this latter has to be actually *flooded* by each $r(k)$ exclusively to its *interfering* nodes, i.e., the ones for which $g(l,k) \neq 0$.

5.2.1 Signalling overhead and scalability

We have formerly pointed out that the DRAA relies on a limited information exchange among interfering links, so that signalling is only established from each receive node to the transmit nodes within its reception range. This means that:

i) when MAI-free orthogonal access is allowed, each transmit-receive pair acts autonomously and the proposed distributed resource allocation collapses into L independent power-control algorithms;

ii) the scalability of the proposed algorithm depends more on the MAI configuration than on the network size;

iii) only highly dense MAI-affected networks are expected to demand large signalling overhead.

Hence, the overall conclusion is that, in the worst case, the information overhead induced by the proposed DRAA scales as $\mathcal{O}(N_I^{max})$, where N_I^{max} is the maximum number of mutually interfering links that are allowed to be simultaneously active over the network.

5.2.2 Adaptive tuning of the stepsize sequence and noisy signalling

Tuning of the stepsize sequence $\{a^{(k)}\}$ in (5.5) should guarantee a suitable tradeoff among the contrasting goals in [81]:

i) fast convergence-speed, when the network is in the stationary regime;

ii) reliable tracking of network changes, when nonstationary events (as, for example, node-failure or fading-variation events) occur;

iii) low implementation-complexity and good numerical stability.

Large stepsizes usually speed up convergence at the cost of poor accuracy. On the other hand, small ones achieve high precision but may require significantly long convergence times. Thereby, a sensible choice could be to adapt the stepsize in order to *quickly* track large networking time-variations and achieving *good* refinements in the steady-state. To this end, the approach in [81] can be applied, where the stepsize in (5.5) is updated according to *both* current and previous gradients as in

$$a_u^{(k+1)} \equiv \min\left\{a_u^{(k)} + \alpha_u \nabla_u^{(k)} \overline{\nabla}_u^{(k)}; a_{max}\right\}, \tag{5.10}$$

where

$$\overline{\nabla}_u^{(k)} \triangleq \left(\epsilon_u \nabla_u^{(k-1)} + (1-\epsilon_u)\overline{\nabla}_u^{(k-1)}\right) \tag{5.11}$$

is a scalar weighted average of past gradients, α_u, ϵ_u are (properly set) small positive constants, and a_{max} is the maximum stepsize guaranteeing numerical stability. By means of (5.10), the stepsize is adjusted according to the trends of the amplitudes of gradients: larger stepsizes will be used whenever there are sudden changes or big variations and smaller ones when approaching the solution.

Another important aspect to be accounted for, in the case of distributed algorithms relying on information exchange, is the effect of noisy signalling. Although such exchange in the DRAA is limited and signalling is usually carried by low-speed, high-reliability feedback channels, there could still be situations in which nodes may receive either noise-affected or stale information. In order to analyze convergence and tracking capability of the distributed algorithm in these scenarios, the noise-affected sample $\widehat{D}_l^{(k)}$ of the signalling information $D_l^{(k)}$ in (5.9) at the k-th iteration is modelled as follows

$$\widehat{D}_l^{(k)} \equiv \sqrt{\rho}\, D_l^{(k)} + \sqrt{1-\rho}\, \sqrt{E\{D_l^2\}}\, \nu_l^{(k)}\,, \tag{5.12}$$

where $\{\nu_l^{(k)}, k = 0, 1, \dots\}$ is a zero-mean, independent and identically distributed (i.i.d.) noise sequence and $\rho \in [0, 1]$ is a parameter that controls the normalized observation-to-noise ratio: $(\rho/(1-\rho))$ affecting the received signalling information. According to (5.12), lower values of ρ correspond to noisier $\widehat{D}_l^{(k)}$, with $\rho = 1$ being the noise-free case.

In this regard, the contribution in [82] shows that, under the (quite mild) technical conditions detailed in [82, Th.3.1, Th.3.2], the presence of observation noise *does not* affect the steady-state values approached by gradient-based iterative algorithms, as the one developed in (5.5)-(5.10). The numerical tests that will be shown in Chapter 6 give explicit evidence that this conclusion holds in the considered framework and prove the robustness of the DRAA against the impairing effects possibly arising from noisy signalling.

5.3 Implementation details

The preceding sections have provided a deep analysis of the algorithmic solution of the subproblems comprising the proposed decomposition.

In detail, Section 5.2 has shown that the DRAA enables each node of the network to independently set up the optimal link-capacities, solutions of the MPOP, by adjusting the resource allocation relying on a limited and, most importantly, entirely local signalling. Furthermore, the DRAA performance has been shown to be rather unaffected by imperfectly received signalling. Roughly speaking, the DRAA works similarly to current power control algorithms so that it can be easily implemented on both the clients and the routers of the network. Overall, these properties allows to consider the ERAP as a problem that each node can cope with autonomously and, therefore, will not be further investigated.

In order to run the DRAA, however, each node needs to be provided with information on links to set up and their capacities. As discussed in Section 5.1, these data can be computed through either a centralized or a distributed approach as part of the FNCP solution. Besides entailing different signalling burden, these techniques may also impact differently on the equipment of the network nodes and on the network protocols so that to properly choose between them requires to be particularly attentive to the considered application scenario.

Since the FNCP computes both the optimal network topology (i.e., through link-capacities) and the traffic distribution, and since common TE approaches (reviewed in Section 1.2.1) apply to capacitated networks, it is important to distinguish these two components of the FNCP solution in considering implementation aspects. In fact, whether the topology is computed by a centralized or a by distributed algorithm, issues related to packet forwarding can be dealt

with separately.

For example, even when the set of link capacities is determined at a central controller and flooded through the network so as to enable optimal resource allocation, it is possible to implement optimal TE equivalently through a connection-oriented solution (such as on MPLS) or by means of a distributed IP-TE solution as the one presented in [13]. This last, in particular, only requires NECMP routing functionalities to the network nodes and no additional protocol stacks.

Chapter 6

Numerical Results

This chapter focuses on the performance evaluation of the proposed Two-Level Decomposition. Several topologies, objective functions (load balancing, flow maximization) and scenarios (unicast, multicast, multisource) have been analyzed and the performance of the MPOP solutions compared with those resulting from more conventional approaches such as: the shortest-path routing, the minimum-cost-tree multicasting and the interference-avoidance. Furthermore, part of this chapter is dedicated to the study of the properties of the DRAA derived in Chapter 5. The presented results underline the good convergence behaviour and the quick reaction (to both node failures and fading variations) exhibited by the DRAA, and give evidence of its noisy-signalling robustness. Practical relevance of Proposition 4.3 is also addressed, and actual effectiveness of its claims is proved. In this regard, it must be underlined that all the numerical results provided in this chapter refer to *exact* solutions of the corresponding MAI-affected nonconvex MPOPs (see Proposition 4.3.3).

$N = 0.01\,\mathrm{mW}$	$\Gamma_{max} = 0.5$	$\eta = 0.8$	Div=1
$G_{min} = 10^{-2}$	$\varepsilon = 1$	$G_{max} = 1$	$H_t = +\infty$

Table 6.1: *Main simulation parameters.*

6.1 Simulation setup

In the carried out numerical tests, the (usual) Shannon-Hartley's logarithmic formula in (4.16):

$$C(l) \equiv B \log_2(1 + \mathrm{SINR}(l)),\ (\mathrm{Mb/s})$$

is adopted to measure the capacity of the l-th link with bandwidth $B \equiv 1$ MHz. The capacity function in (4.16) meets all the assumptions on $\Psi_l(\cdot)$ reported in Section 3.1 and guarantees *nonnegative* capacity-values, even for *vanishing* SINRs. The polyhedral capacity region outer-bound derived in Section 4.3.1 is employed throughout all simulations, with $\overline{\Psi}_{k,l}(\cdot)$ in (4.15) given by (4.18).

The exponential relationship in (3.10) with $a_i = 1$ and $b_i = c_i = 0$ is measures the per-session media distortion, while the following link-power summation: $\sum_l P(l)$ is considered as the ERAP cost function in (4.5.1). Parameters of the DRAA gradients updates in (5.10) have been set to $a_{max} = 0.4, \alpha_u \equiv 10^{-5}$ and $\epsilon_u \equiv 10^{-6}$.

Unless otherwise stated, the basic set of system parameters for the numerical results is specified in Table 6.1. Lacking system parameters (such as QoS requirements, power budget and so on) will be detailed, together with network topologies and interference configuration, for each addressed scenario.

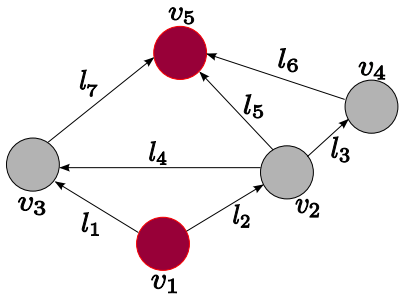

Figure 6.1: *Hierarchical network topology.*

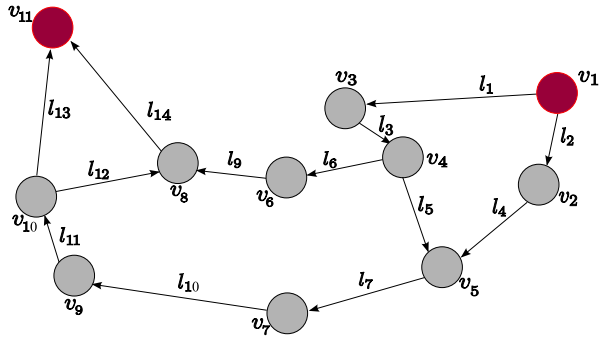

Figure 6.2: *Abilene network topology.*

6.2 Unicast

The first performance analysis is centered on a single-class unicast case. Both the simple hierarchical network topology in Figure 6.1 [41] and the Abilene network in Figure 6.2 [74] have been considered. Single-session average queueing-plus-transmission delay in induced by the l-th link is measured by

$$\Delta(C(l), x(l)) \equiv [C(l) - x(l)]^{-1} + C(l)^{-1} \ (\mu\text{s}). \tag{6.1}$$

Comparisons with (conventional) shortest-path *non-bifurcated* (i.e., single-path) routing algorithms, that adopt suitable path-metrics for reflecting the consid-

ered QoS parameters, is carried out. For this purpose, the basic Destination-Sequenced Distance-Vector (DSDV) routing algorithm in [14] has been implemented, with metric $\widehat{cm}_l$ for the l-th link set to (see [17,83])

$$\widehat{cm}_l \triangleq AP(l) + B\Delta(C(l), x(l)),\ l = 1, \ldots, L, \tag{6.2}$$

where $P(l)$ (mW) is the power radiated by $t(l)$, and $A \triangleq 0.5$ mW^{-1}, $B \triangleq 0.5\ \mu$s^{-1} are dimensioned constants. In principle, the (nonnegative and dimensionless) link-metric in (6.2) is able to capture the tradeoff between total radiated power and resulting path-delay, typically present in wireless networking scenarios supporting delay-sensitive media applications.

6.2.1 Load balancing capability

Topology in Figure 6.1 may be somewhat representative of access WMNs, where the number of nodes in each tier decreases as we move from the source-node v_1 (e.g., a mesh client) to the destination-node v_5 (e.g., a gateway node for the wired Internet access). The basic system parameters for these tests are collected in Table 6.1. Nonuniform resource distribution is considered so that $G_{max}(1) = G_{max}(7) = 0.9$, $C_{max}(1) = 3$ Mb/s, $C_{max}(7) = 4$ Mb/s, $C_{max}(2) = 4$ Mb/s, whereas for all the other links $C_{max} = 5$ Mb/s. Each node has a power budget of $P_{max} = 2$ mW, and $C_{ave} = 20$ Mb/s. QoS requirements are set to: $\nabla_t = 8\ \mu$s, $\sigma_D^2 = 0.2$ and $B_{min} = 2$ Mb/s. Interfering links have been assumed to be those not sharing a transmit or a receive node and not belonging to the same path, and G_{min} in Table 6.1 indicates their minimum allowed gain[1].

Figure 6.1 shows that the available paths are: the two-hops $\mathcal{P}_1 \triangleq \{v_1 \rightarrow v_3 \rightarrow v_5\}$ and $\mathcal{P}_2 \triangleq \{v_1 \rightarrow v_2 \rightarrow v_5\}$; and the three-hops $\mathcal{P}_3 \triangleq \{v_1 \rightarrow v_2 \rightarrow v_3 \rightarrow v_5\}$, and $\mathcal{P}_4 \triangleq \{v_1 \rightarrow v_2 \rightarrow v_4 \rightarrow v_5\}$. Since these paths are

[1]Mutually orthogonal links exhibit vanishing interfering gains.

β	Div	$\mathcal{P}_1$		$\mathcal{P}_2$		$\mathcal{P}_3$		$\mathcal{P}_4$		f
		flow	delay	flow	delay	flow	delay	flow	delay	
2	0.9	0.84	1.36	0.99	1.05	0.00	0.00	0.17	3.12	2.00
	0.5	1.00	1.42	0.86	1.02	0.00	0.00	0.14	3.08	2.00
16	0.9	0.97	1.41	0.54	1.12	0.00	0.00	0.49	2.74	2.00
	0.5	1.00	1.42	0.52	1.11	0.00	0.00	0.48	2.73	2.00

Table 6.2: *Numerical results for the Hierarchical topology in Figure 6.1. Flows are in (Mb/s) and delays are in (μs). The shadowed row indicates the most performing obtained solution.*

partially overlapping, this topology appear as a good test for the load balancing capability of the considered objective function of the MPOP.

Table 6.2 reports the numerical MPOP solutions obtained by considering the objective function in (3.8) with $\theta = 0.5$ and $\alpha = 1$ for some values of the parameters β, Div in (3.8), (3.6.4). Specifically, each row of Table 6.2 reports the path-flows (in Mb/s) and path-delays (in μs), together with the resulting end-to-end forwarded flow f. An analysis of these numerical results allows to draw three main conclusions about the performance of the proposed resource allocation algorithm. First, more load-balanced traffic patterns are attained for increasing values of the β exponent in (3.8) and/or decreasing values of Div. Second, the resulting values achieved for the aggregate forwarded flow are almost unsensitive to β and Div, at least for Div values ranging over the interval $[0.5, 0.9]$. Third, the achieved maximum path-delay decreases as more load-balanced traffic patterns (that is, for increasing β and decreasing Div values) are considered.

	$\mathcal{P}_1$	$\mathcal{P}_2$	$\mathcal{P}_3$	$\mathcal{P}_4$
delay	4.80	4.80	7.20	7.20
cost	2.50	2.49	3.75	3.75

Table 6.3: *Path-delays (μs) and path-costs of the DSDV routing for the network in Figure 6.1. The shadowed column indicates the most performing DSDV-based solution.*

$P_{max} = 3\,\text{mW}$	$\sigma_D^2 = 0.3$
$\nabla_t = 15\,\mu\text{s}$	$C_{ave} = 100\,\text{Mb/s}$
$B_{min} = 4.8\,\text{Mb/s}$	$C_{max} = 5\,\text{Mb/s}$

Table 6.4: *Simulation parameters for the Abilene network in Figure 6.2.*

6.2.2 Shortest-path comparison

The MPOP performance has been compared to the one of the DSDV algorithm for both the network topology in Figures 6.1 and 6.2. In the case of the former, the flow-demand $\widehat{f}$ required to the DSDV routing algorithm *coincides* with the aggregate flow $f = 2$ Mb/s carried by the MPOP with $\beta = 16$ and $Div = 0.5$ (see the 4-th row of Table 6.2). This is done to give rise to a fair performance comparison. End-to-end path delays (μs) and path-costs entailed by the four available paths are collected in Table 6.3. The DSDV shortest-path, $\mathcal{P}_2$, presents a delay of 4.8 μs that almost doubles the one resulting from the MPOP, which is (see the last row of Table 6.2) of 2.73 μs. Therefore, in the considered networking scenario, the delay gain arising from the multipath-nature of the proposed cross-layer resource allocation solution is about 55%.

DSDV shortest-path routing performance has been assessed also in the case

	node-composition	DSDV			MPOP	
		power (mW)	delay (μs)	cost	delay (μs)	flow (Mb/s)
$\mathcal{P}_1$	$\{1,3,4,6,8,11\}$	n.f.	n.f.	n.f.	4.96	3.57
$\mathcal{P}_2$	$\{1,3,4,6,7,9,8,11\}$	11.03	8.00	9.51	0.00	0.00
$\mathcal{P}_3$	$\{1,3,4,6,7,9,10,11\}$	n.f.	n.f.	n.f.	0.00	0.00
$\mathcal{P}_4$	$\{1,3,4,5,7,9,10,8,11\}$	10.17	8.00	9.08	0.00	0.00
$\mathcal{P}_5$	$\{1,3,4,5,7,9,10,11\}$	n.f.	n.f.	n.f.	0.00	0.00
$\mathcal{P}_6$	$\{1,2,5,7,9,10,8,11\}$	9.74	7.00	8.37	0.00	0.00
$\mathcal{P}_7$	$\{1,2,5,7,9,10,11\}$	n.f.	n.f.	n.f.	6.59	1.23

Table 6.5: *Power consumption, path-delays and path-costs of the DSDV routing vs. flows and delays of the MPOP multipath solution for the network in Figure 6.2. The shadowed row indicates the performance of the best path computed by the DSDV algorithm.*

of the network in Figure 6.2, where the source v_1 sends data do the destination v_{11}. Basic simulation parameters for the Abilene network are detailed in Table 6.4. Interfering links are assumed to be those ending in the same receive node, and nonuniform resource availability is considered: links indexed by 4, 6, 9, 13 having $[G_{max}, C_{max}\ (Mb/s)]$ equal to [0.3, 3], [0.3, 3], [0.2, 2 and [0.1, 1], respectively. Again, in order to perform a fair comparison, both the MPOP and the DSDV algorithms are required to support the same flow $f = B_{min}$ and the DSDV link cost takes into account both delay and power consumption, according to (6.2).

The obtained numerical results in Table 6.5 show that, because of the node power limitations, a subset of the possible paths (whose node composition is detailed in the Table) fails to guarantee the minimum bandwidth and it is, therefore, marked as "not feasible" (n.f.). The DSDV best path (i.e., path $\mathcal{P}_6$) entails a cost equal to 8.37, whereas the MPOP solution, since the network total

power is 6.70 mW and the worst delay is 6.59 μs, gives rise to a cost equal to 6.65. These results prove that, in the considered application, the multipath routing enabled by the MPOP allows to save almost the 31% of power, while even gaining the 4% in delay.

6.2.3 MAI-free multipath routing comparison

The presented performances of the DSDV routing algorithm are also the *best* attainable by a *single-path* routing algorithm when conflict-free scheduling is implemented at the MAC layer of the networks. However, since the MPOP gain can arise from being a multipath solution besides an interfered-one, it might be interesting to evaluate the performance of a multipath routing algorithm that implement *conflict-free* scheduling policies attaining MAI-free transmissions over the network.

For this purpose, according to [39], all possible subgraphs of the network in Figure 6.1 that allow the implementation of conflict-free link-activations have been enumerated[2]. By applying the MPOP with maximum flow objective function, i.e., $\Phi\left(f, \overrightarrow{x}, \overrightarrow{C}\right) \equiv -f$, to each conflict-free subgraph, it can be ascertained that the highest flow subgraph comprises of links 2, 3, 5, 6. Its total conveyed flow is 3.2 Mb/s with maximum path-delay 2.6 μs for a power consumption of 1.36 mW. Application of the MPOP on the complete network-graph (that is, considering the potential simultaneous activation of interfering links), on the contrary, results in a total flow of 5 Mb/s a maximum delay of 2.38 μs and a total power consumption equal to 1.30 mW. This means that with the same power budget and even less delay it is has been possible to reach a 30% higher throughput with respect to the interference-avoidance case. The

[2]It is well known that the enumeration of all conflict-free subgraphs is NP-hard [39]. Nonetheless, the size of the network in Figure 6.1 is such that this enumeration is still possible.

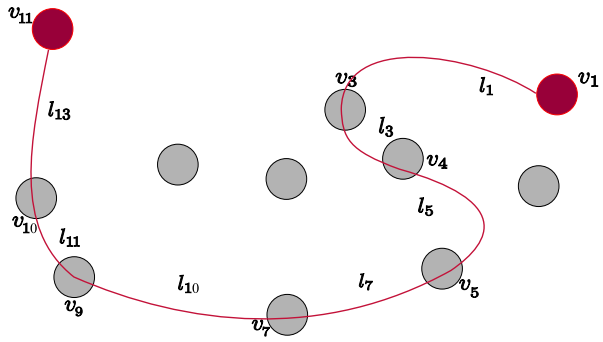

(a) Conflict-free

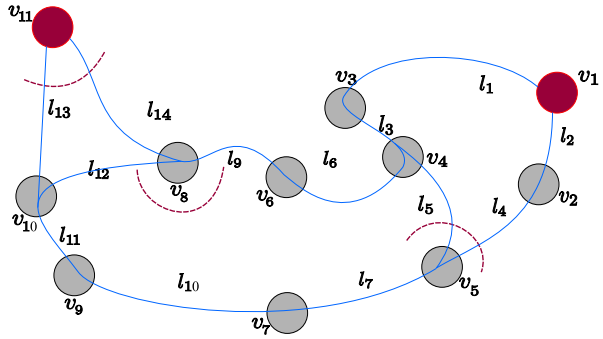

(b) Interfered

Figure 6.3: *Abilene network maximum-flow MPOP solutions. Red-dashed arches indicates interfering links.*

same analysis has been carried out for the Abilene network. Figure 6.3 shows the maximum-flow conflict-free graph (a) and the maximum-flow interfered (b) solution. Conveyed flows of these last are 3.99 Mb/s and 6.40 Mb/s, respectively, meaning that the performance gain of the interfered solution is up to the 60%.

These results support that, in power-limited scenarios and when the MAI affecting the links is not too high, interference-avoiding multipath routing strate-

gies, in addition to entailing burdensome exponential complexity [39], can *fail* to reach the maximum end-to-end flow. In these operating conditions, in fact, allowing a residual MAI can induce the activation of mutually interfering links and give rise to better performance.

6.3 Multisession multicast

In this set of numerical test, the case of multiple multicast sessions with intra-session NC is investigated. In particular, goals of this section are to:

i) evaluate the NC multicast throughput gain of the MPOP with respect to its routing-based counterpart;

ii) compare the performance (in terms of both total power consumption and incurred per-session delay) of the proposed algorithm with the one given by Dense Mode-Protocol Independent Multicast (DM-PIM) based solutions;

iii) show how the MPOP is capable to differentiate the resource allocation in order to comply with QoS requirements of separate session.

Being a multisession scenario, in order to measure the average queueing-plus-transmission delay in (3.6.9) induced by link l on the i-th session flow, the following convex delay function (measured in s) is adopted:

$$\Delta_i(C(l), x_1(l), \ldots, x_{_F}(l)) \equiv \frac{1}{C(l)} + \frac{\eta(l)}{C(l) - x_i(l) - 2\left(\sum_{m=1}^{i-1} x_m(l)\right)}\,. \quad (6.3)$$

Appendix B proves that such function abides by the assumptions given in Section 3.1 and is a (convex) upper bound on the actual per-link average delay induced by M/M/1 nonpreemptive queueing systems with F different priority classes. Furthermore, it converges to the actual average delay of [67, Sect.3.5.3] when link l is lightly loaded (e.g., for vanishing values of the link utilization coefficients: $\{x_i(l)/C(l), 1 \leq i \leq F\}$).

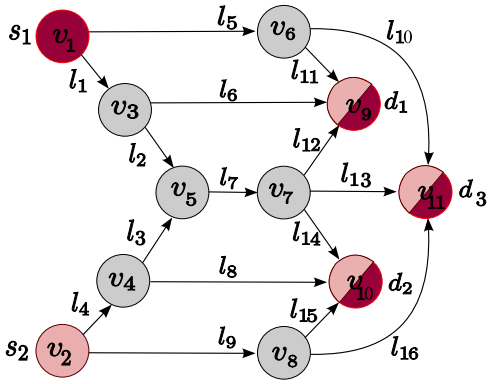

Figure 6.4: *Butterfly network topology.*

$P_{max} = 2\,\text{mW}$	$\sigma_D^2 = 0.2$
$C_{ave} = 50\,\text{Mb/s}$	$\nabla_t = 30\ \mu\text{s}$
$C_{max} = 4\ \text{Mb/s}$	$B_{min} = 2\ \text{Mb/s}$

Table 6.6: *System parameters for the butterfly network in Figure 6.4.*

6.3.1 Network coding gain

The butterfly-shaped network topology in Figure 6.4 [53], where two sessions belonging to the *same* QoS class are active is considered. The session sources, s_1 and s_2 (located ad v_1 and v_2, respectively) have a common destination set: $\mathcal{D}_1 \equiv \mathcal{D}_2 = \{d_1, d_2, d_3\}$. Main simulation parameters are detailed in Table 6.6. Interfering links are considered to be the ones ending into a common receive node, and, again, the G_{min} entry in Table 6.6 indicates their minimum interfering gain. Nonuniform resource availability is considered: differently from the others, links indexed with 5, 6, 7, 8 and 9 in Figure 6.4 are characterized

Sink	Path	node-composition	Flows (v_6, v_8 ON)		Flows (v_6, v_8 OFF)	
			R	NC	R	NC
d_2	$\mathcal{P}_1$	$\{v_2, v_8, v_{10}\}$	0.95	2.40	0.00	0.00
	$\mathcal{P}_2$	$\{v_2, v_4, v_{10}\}$	0.58	2.40	1.00	1.61
	$\mathcal{P}_3$	$\{v_2, v_4, v_5, v_7, v_{10}\}$	0.07	0.00	0.00	0.37
	$\mathcal{P}_4$	$\{v_1, v_3, v_5, v_7, v_{10}\}$	1.60	2.45	1.00	1.22
d_3	$\mathcal{P}_5$	$\{v_2, v_8, v_{11}\}$	1.40	2.40	0.00	0.00
	$\mathcal{P}_6$	$\{v_2, v_4, v_5, v_7, v_{11}\}$	0.20	1.22	1.00	1.60
	$\mathcal{P}_7$	$\{v_1, v_6, v_{11}\}$	1.40	2.40	0.00	0.00
	$\mathcal{P}_8$	$\{v_1, v_3, v_5, v_7, v_{11}\}$	0.20	1.22	1.00	1.60
		Multicast Flow f	3.20	7.25	2.00	3.20

Table 6.7: *Path-flow distributions to destinations d_2, d_3 for the application scenario of Section 6.3.1. All flows are measured in (Mb/s). Being the topology in Figure 6.4 symmetrical, path-flows to d_1 coincide with the ones to d_2*

by $C_{max} \equiv 5$ Mb/s. Furthermore, a single QoS-class is considered, so that $f_1 = f_2 \equiv f$ and the (common) value of the bandwidth and delay requirement of each session are fixed to the B_{min} and ∇_t values in Table 6.6.

Let us analyze the flows distribution when: *i)* the objective function in (4.4.1) is the total flow arriving at each destination, i.e., $\Phi\left(\overrightarrow{f}, \overrightarrow{x_1} \ldots, \overrightarrow{x_F}, \overrightarrow{C}\right) \equiv -f$; and, *ii)* the resulting MPOP is solved either by routing (i.e., as a *multiple* unicast problem, see Section 3.3.1) or by applying intra-session network coding. The available paths to the sinks d_2, d_3, their nodes composition and the corresponding Routing-based (R) and Network Coding-based (NC) flows (in Mb/s) are detailed in the first four columns of Table 6.7. The reported values point out the gain in the multicast throughput arising from NC: in fact,

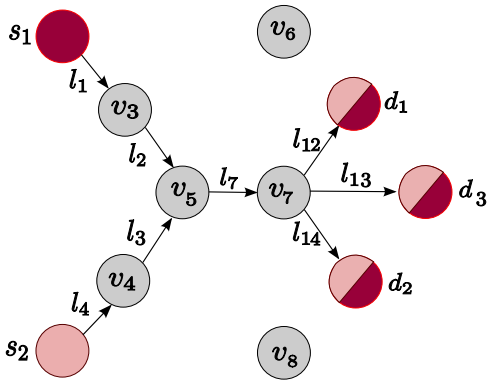

Figure 6.5: *Minimum-hop distribution tree of the butterfly network in Figure 6.4.*

the multicast flow $f_{NC} = 7.25$ Mb/s sustained by the NC solution *more than doubles* the routing one f_R, which is only equal to 3.20 Mb/s.

Moreover, as shown in the last two columns of Table 6.7, network coding is *still* beneficial when node failures occur. However, since node failures generally make the number of available source-destination paths decrease, in this case the throughput gain due to NC over the multipath routing solution is limited up to 37% when the nodes v_6, v_8 in Figure 6.4 go down.

6.3.2 DM-PIM comparison

Since computing the optimal Steiner trees is an NP-hard problem (see [32] and references therein), in order to carry out meaningful performance comparisons with routing-based (i.e., without NC) multicast algorithms of practical interest, the DM-PIM in [84] is considered. This solution multicasts sessions-information over the *minimum-hop* (i.e., shortest-path) distribution trees. To this end, all simulation parameters in Table 6.6 have been kept unchanged, and

$P_{max} = 3\,\mathrm{mW}$	$B_{min}(2) = 2\,\mathrm{Mb/s}$
$C_{ave} = 100\,\mathrm{Mb/s}$	$\nabla_t(2) = 60\ \mu\mathrm{s}$

Table 6.8: *Simulation Parameters for the SPRINT topology in Figure 6.6.*

both the proposed and the implemented DM-PIM algorithms are required to support the same multicast flow $f = 2$ Mb/s to each intended destination.

In this scenario, it has been numerically ascertained that the minimum-hop distribution tree built up by the DIM-PM algorithm over the butterfly network, which is shown in Figure 6.5, entails a total power consumption and a maximum delay equal to 2.88 mW and 7.2 μs, respectively. The corresponding values for the MPOP solution are: 0.72 mW and 5.57 μs. Comparison of the reported values proves that, by performing a more even distribution of the multicast flows over the available paths, the MPOP is able to save more than the 75% of power (even with a 6% delay-gain) with respect to the DM-PIM-based resource allocation, whose target is the minimization of the number of utilized links.

6.3.3 Multi-QoS multisession multicast

Let now analyze the MPOP solutions when sessions belonging to *different* service classes are present. For this purpose, the so-called SPRINT network [22] in Figure 6.6 with the system parameters in Table 6.8 is considered. Each link has equal maximum capacity set to $C_{max} = 6$ Mb/s. The two active multicast sessions have different sources $\{s_1 = v_1, s_2 = v_2\}$ and partially overlapping destination sets: $\mathcal{D}_1 \equiv \{v_{13}, v_{14}\}$ and $\mathcal{D}_1 \equiv \{v_{14}, v_{15}\}$.

Table 6.9 shows the delays and the power consumption resulting from the different QoS requirements. From the presented results, it is clear that in the presence of unbalanced QoS-requirements, the experienced quality of each ses-

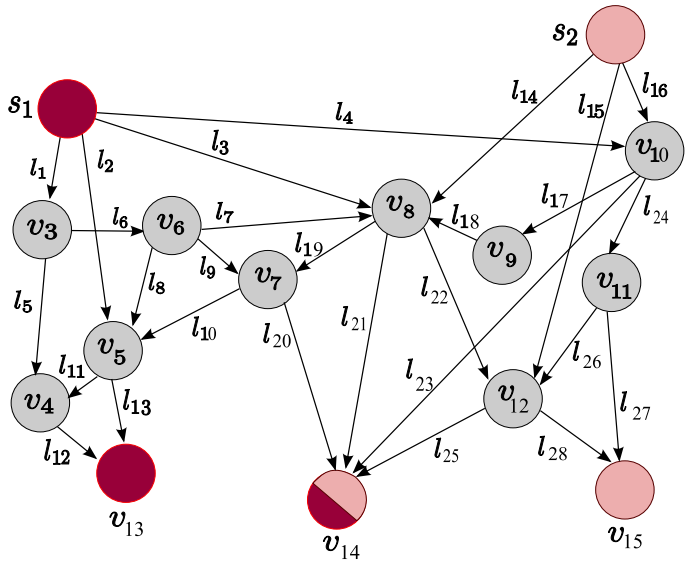

Figure 6.6: *SPRINT network topology.*

sions is significantly different. For example, when session S_1 decreases its maximum delay from 60 to 15 μs (see column 2 and 3 of Table 6.9), the corresponding delay becomes three times lower than the one of session S_2. Obviously, stricter requirements induce higher power consumption, for the capacity of the network links has to increase (see last row of Table 6.9). In detail, guaranteeing both higher rate and lower delay to S_1 drives the network from a total power of 0.64 mW to 9.94 mW, which in more than 10 times higher.

6.4 Multisource multicast

In this section, the Multisource MPOP formulated in Section 3.3.2 is investigated. In addition to showing how the MMPOP is able to take into account

	$B_{min}(1) = 2$ Mb/s		$B_{min}(1) = 5$ Mb/s	
	$\nabla_t(1) = 60\mu$s	$\nabla_t(1) = 15\mu$s	$\nabla_t(1) = 60\mu$s	$\nabla_t(1) = 15\mu$s
Delay S_1 (μs)	42.17	9.53	43.94	10.42
Delay S_2 (μs)	48.51	31.97	47.12	32.85
P_{tot} (mW)	0.64	3.51	2.72	9.94

Table 6.9: *Total delays and power consumptions for different per-session QoS requirements.*

$P_{max} = 4\,\text{mW}$	$C_{max} = 8\,\text{Mb/s}$
$H(S_1) = 2\,\text{Mb/s}$	$\nabla_t = 50\ \mu\text{s}$

Table 6.10: *Simulation parameters for the butterfly network in Figure 6.4 and the scenario in Section 6.4.*

the potential correlation of the sources and to leverage on both NC and Source Coding (SC) to enhance the system performance, the presented numerical results will also address the effects of increasing MAI levels and of stricter quality requirements.

To this end, the butterfly-shaped network topology in Figure 6.4 is considered, where, again, two sessions belonging to the *same* QoS class are active. Simulation parameters are detailed in Table 6.10, and the interference configuration is the same as in Section 6.3.1: interfering links are considered to be the ones ending into a common receive node. Furthermore, sources are assumed to generate discrete time, quantized sequences of independent (in the time domain) identically distributed (i.i.d.) symbols according to a given joint probability distribution, that accounts for the inter-source spatial correlation. According to [56], the source nodes encode their flows independently, i.e., *with-*

		$H(S_1\|S_2)$ (Mb/s)				
		2.00	1.50	1.00	0.50	0.00
Delay (μs)	NC	32.14	25.92	21.60	14.75	14.23
	DM-PIM	14.40	11.52	9.60	8.22	7.20

Table 6.11: *Maximum path delays for the scenarios in Section 6.4.*

out resorting to any inter-source message passing, and they present symmetric entropies, i.e., $H(S_1) = H(S_2)$ (bit/s).

Once more, MMPOP performance are along with the ones resulting from a conventional DM-PIM based resource allocation policy. Figure 6.7 reports the power consumption of the MMPOP and the DM-PIM solutions when the conditional entropy $H(S_1|S_2)$ varies in the range $[0, H(S_1)]$ in the case of low MAI, i.e., for G_{min} =0.01. The plots in Figure 6.7 show that NC guarantees better performance even when the source are independent (i.e., when $H(S_1|S_2) = H(S_1)$) and the flow to the destinations grows from 2 Mb/s to 4 Mb/s. Moreover, in this case, the power gain of NC with respect to DM-PIM reaches the 66%. A similar scenario is depicted in Figure 6.8, where a MAI level ten-times higher (i.e., G_{min} =0.1) is considered. NC is still beneficial in this high-interfered case but when the sources are independent.

Table 6.11 shows how the maximum delays resulting from the two strategies varies as a function of $H(S_1|S_2)$: to lower values of $H(S_1|S_2)$ correspond lower delays since the links have to carry minor flows.

Finally, to take into account traffic sessions belonging to *different* quality requirements, the SPRINT network scenario depicted in Section 6.3.3 is considered with the same system parameters of Table 6.10 where $\nabla_t(2) = \nabla_t$. Again, the two sources are symmetric with $H(S_1) = H(S_2)$. In Figure 6.9 the impact of different delay requirements on the network power consumption,

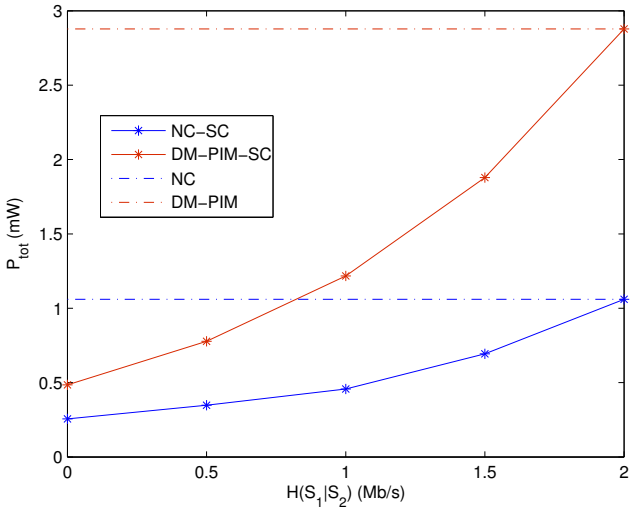

Figure 6.7: *Total power consumption in the presence of NC, SC and comparison with DM-PIM, for several values of $H(S_1|S_2)$. Case of low MAI.*

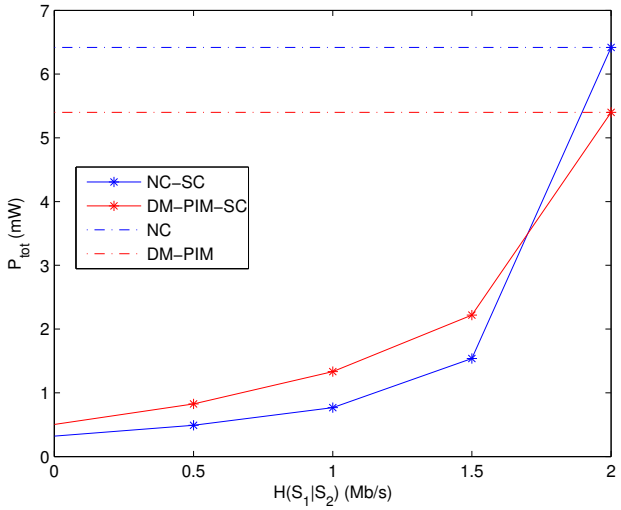

Figure 6.8: *Total power consumption in the presence of NC, SC and comparison with DM-PIM, for several values of $H(S_1|S_2)$. Case of high MAI.*

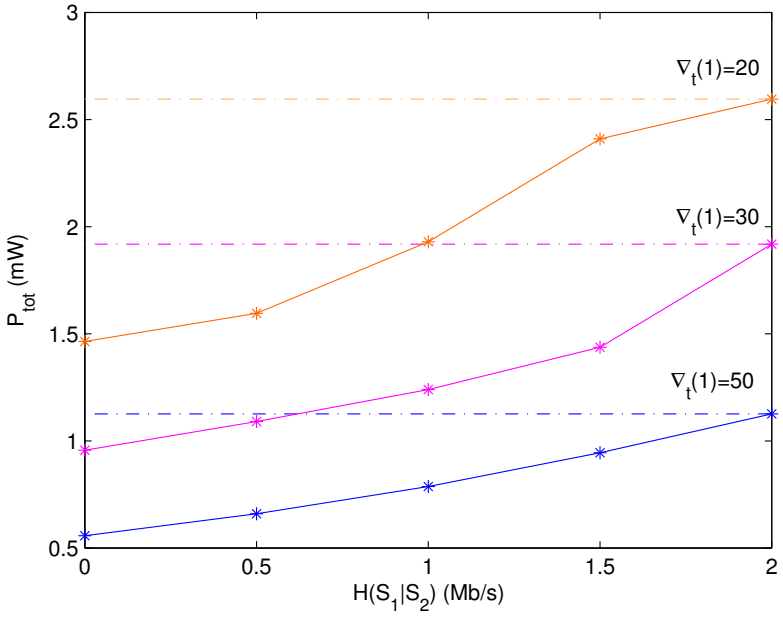

Figure 6.9: *Total power consumption in the presence of NC, SC for several values of* $H(S_1|S_2)$ *and* $\nabla_t(1)$ *(*μs*).*

for various values of $H(S_1|S_2)$ is reported. From the plots, it stems out that the stricter the first session maximum delay, the higher the power required by the network. This happens because lower delays can significantly increase the capacity needed at the network links. In the tested cases, lowering the maximum delay from 50 μs to 20 μs increases the network power utilization from 1.19 mW to 2.62 mW in the case of $H(S_1|S_2) = H(S_1)$, and from 0.55 mW to 1.48 mW in the case of $H(S_1|S_2) = 0$, which means that, depending on actual inter-source correlation, halving the delay requirement may result in $50 - 60\%$ higher power consumptions.

6.5 Convergence, adaptivity and robustness of the DRAA

Being an iterative distributed algorithm, the DRAA's convergence behaviour and its adaptivity to variations in the operating conditions (e.g., node-failure events and/or fading-induced fluctuations of link gains) need to be further analyzed. To this end, in this section the flow time-evolutions of some of the previously-reported scenarios are provided. In all the reported figures, time is expressed by the algorithm iteration index k.

Figures 6.10 and 6.11 refer to the butterfly topology described in Section 6.3 on Multisession Multicasting. The convergence behaviour and the adaptivity to node failures of the DRAA of Section 5.2 along with the effects of noisy signalling may be appreciated through an examination of the plots in Figure 6.10. These latter report the time-evolution of the total flows f_{NC} and f_R defined in Section 6.3.1 to the sink d_2 for some (decreasing) values of the noise-parameter ρ in (5.12), with $\rho = 1$ being the error-free case.

Good convergence to the optimal MPOP solutions (indicated by the horizontal lines in Figure 6.10) is achieved within 50 iteration cycles, whereas quick reactivity with respect to node failures (which occur at $k = 200$) is supported by the fact that the optimum is approached (with an error below 10%) within 20 iterations. Moreover, the noise effects on both the convergence speed and the accuracy in the steady-state of the performance of the presented algorithm are nearly negligible, even at values of ρ as low as 0.5.

In order to effectively cope with the time-varying nature of fading-affected channels, iterative algorithms have to converge within the coherence time of the underlying network topology. The plots presented in Figure 6.10 suggest that the proposed algorithm is also capable of very quick reaction to *fading-induced variations*, since they entail less abrupt changes with respect to node failures.

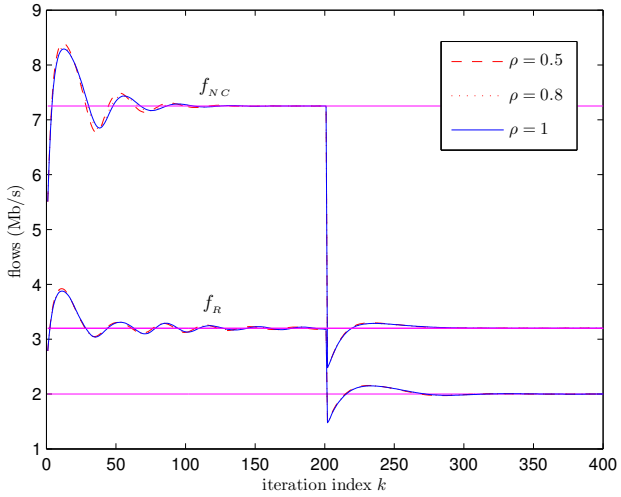

Figure 6.10: *Time-evolutions of routing (f_R) and network coding (f_{NC}) flows to destination d_2, in the presence of failures of v_6 and v_8 at $k = 200$, for several values of the noise parameter ρ.*

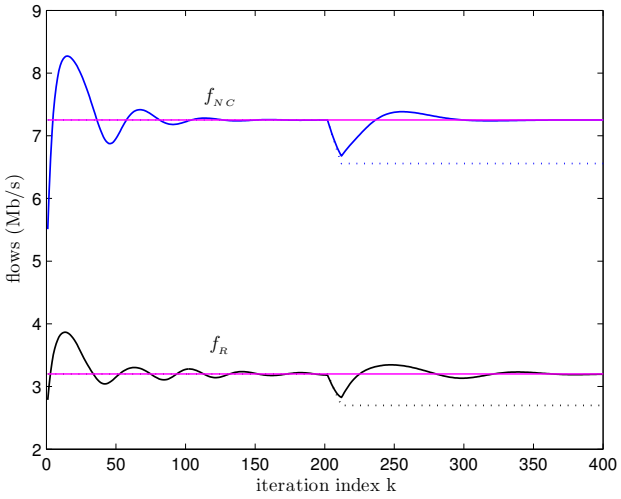

Figure 6.11: *Time-evolutions of routing (f_R) and network coding (f_{NC}) flows to destination d_2, in the presence of a 10% link-gain variation per iteration.*

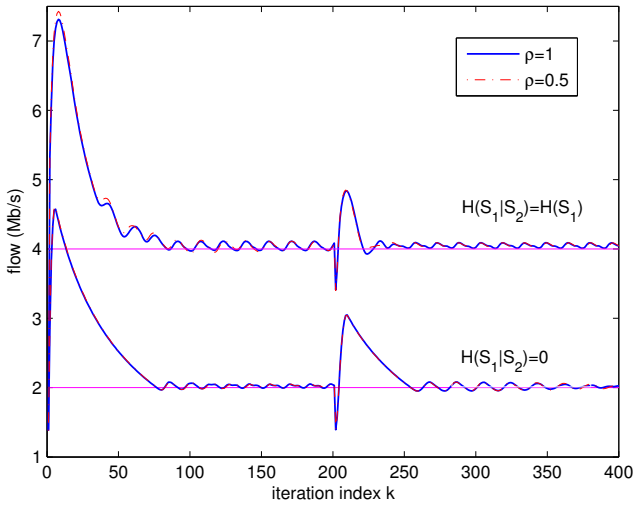

Figure 6.12: *Time-evolutions of flows to destination d_2, in the presence of failure of v_7 at $k = 200$, for several values of the noise parameter ρ and $H(S_1|S_2)$.*

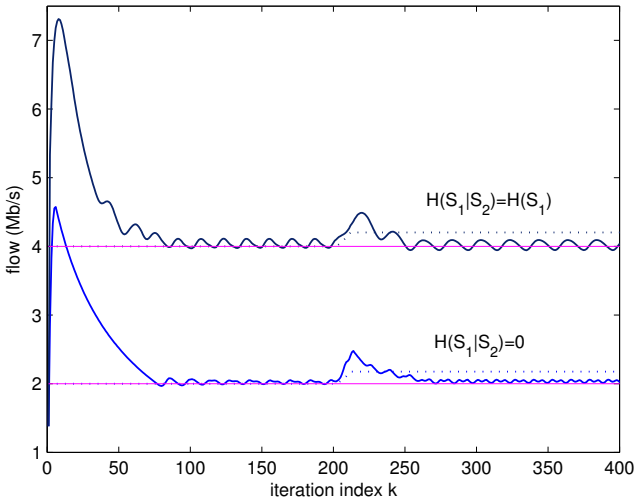

Figure 6.13: *Time-evolutions of flows to destination d_2, in the presence of a 10% link-gain variation per iteration for several values of $H(S_1|S_2)$.*

To support this conclusion, in Figure 6.11 are reported the time-behaviour of the flows of the previous example, when starting from the 200-th iteration, the maximum gains of links 8, 14 and 15 change (with a 10% variation per iteration) from the values in Table 6.6 to $G_{max}(8) = 1.2$, $G_{max}(14) = 0.8$ and $G_{max}(15) = 0.5$.

The dashed plots in Figure 6.11 refer to the corresponding behaviour of flows f_{NC} and f_R when the resource allocation remains the one set for $k < 200$: as a consequence of the channel gains variation, both flows decrease. On the contrary, the solid plots in Figure 6.11 show how the proposed self-adaptive resource management algorithm is able to *successfully* counterbalance link variations, so as to reduce their effects to the upper layers of the implemented protocol stack.

A similar analysis can be performed also in the case of the Multisource Multicast in Section 6.4. For the plots in Figure 6.12 and 6.13 a higher α_{max} has been set. These plots are the Multisource counterpart of the ones in the previous test: they report the time-evolution of the total flow to d_2 of the butterfly network but for the cases of $H(S_1|S_2) = 0$ and $H(S_1|S_2) = H(S_1)$, and for several noise-parameter ρ. Again, the optimal MMPOP solutions converge in less than 100 iterations, and react to the failure of node v_7 at $k = 200$, by approaching the new optimal allocation within 20 iterations.

As to fading variations, the plots presented in Figure 6.13 shows the flow values when, as in the previous example, at $k = 200$, the maximum gains of links 8, 14 and 15 change (with a 10% variation per iteration) from the values in Table 6.6 to $G_{max}(8) = 1.2$, $G_{max}(14) = 0.8$ and $G_{max}(15) = 0.5$, respectively. Comparison of the solid and the dotted plots in Figure 6.13, which refer to the values assumed by f in the case of adaptive and nonadaptive DRAA, respectively, show the DRAA adjusts the power allocation to the new conditions.

Convergence and the adaptivity of the DRAA are dependent on the particular choice of stepsize update (see Section 5.2.2). Even if, in the presented results, both values of α_{max} have proved to guarantee the numerical stability of the algorithm, the higher value, whose effect is shown in Figures 6.12-6.13, affect the performance of the DRAA in the number of iterations to convergence. With respect to the plots in Figures 6.10-6.11, in fact, the ones in Figures 6.12-6.13 show deeper slopes and larger oscillations in the steady-state, suggesting the importance of a proper setup of the stepsize-update parameters.

6.6 Tests of Proposition 4.3

Actual relevance of Proposition 4.3 has been tested by showing how for the butterfly network in Figure 6.4, variations in the system parameters in Table 6.10 impact on the occurrence of the three cases detailed in Proposition 4.3 and give rise to the four cases reported in Table 6.12.

Specifically, if too demanding per-session QoS requirements (such as $\nabla_t(1) = \nabla_t(2) = 10$ μs) are advanced, the corresponding $\mathcal{C}_0$-relaxed FNCP results to be unfeasible (Case A of Table 6.12), and, as was stated in Proposition 4.3.1, so the MMPOP. This also happens when the source entropies are high (e.g., $H(S_1) = H(S_2) = 4$ Mb/s), but their correlation is such that application of source coding is not able to reduce the corresponding session flows, e.g., when $H(S_1|S_2) \simeq H(S_1)$.

MAI-free (Case B in Table 6.12) as well as medium MAI (Case C of Table 6.12: $G_{min} \leq 0.1$) operating conditions guarantee the feasibility of the MMPOP and the *optimality* of the solution derived by the proposed approach (see Proposition 4.3.3).

Finally, when the interference gains grow beyond 0.2 (Case D of Table 6.12), the capacity solution of the $\mathcal{C}_0$-relaxed FNCP, i.e., $\overrightarrow{C}_0^*$, leads to the unfeasibility

Case A	$\mathcal{C}_0$-FNCP unfeasible	MMPOP unfeasible
Case B	MAI-free	MMPOP feasible
Case C	medium MAI	MMPOP feasible
Case D	high MAI	MMPOP undetermined

Table 6.12: *Example of practical relevance of Proposition 4.3.*

of the corresponding ERAP. This means that: either the power constraints are too strict (power-limited scenario) or the outer bound $\mathcal{C}_0$ in (4.15) is too loose (interference-limited scenario).

In the former case, the MMPOP is unfeasible and, in principle, a solution may be found by increasing the P_{max}. The other case imply that, since the employed outer-bound is not tight enough to the actual capacity region, there is no possibility to draw any firm conclusion about actual feasibility/unfeasiblity of the MMPOP, according to Proposition 4.3.2.

Chapter 7

Conclusions

Traffic Engineering for wireless networks is particularly challenging due to the characteristics of the wireless medium. In most cases, in fact, the optimal design of wireless networks results in problems entailing intractable complexity due to the presence of Multiple Access Interference (MAI). Although some instances of this problem have been shown in Literature to admit convex formulation (and therefore to be conveniently solvable with known optimization methods), this conclusion does not hold for the general, and most common, scenario.

This thesis have tackled the optimal flows and resource allocation of a MAI-affected wireless networks where multiple multicast sessions have different QoS-requirements. By means of the proposed Multicast Optimization Problem (MPOP), session utilities, flow control, QoS differentiation, intra-session network coding, MAC design and power-control can be jointly optimized in an integrated framework. To overcome the complexity caused by the nonconvex structure of the MPOP, a two-level decomposition has been devised, which is able to lead to the global optimum of the MPOP by solving two convex subproblems. Sufficient conditions for the optimality of the decomposition solution

are derived along with sufficient conditions for the feasibility of the MPOP.

The solution capability of the proposed decomposition has been shown to be closely related to the tightness of the employed outer-bound of the capacity region to the actual one. Nonetheless, since computation of the tightest capacity region outer-bound may result in a problem as complex as the original, a procedure to devise simple polyhedral outer-bounds has been developed. Important properties of the produced polyhedral bounds is that they: take into account the interference configuration; are asymptotically exact in the case of low MAI; depict the convex hull of the capacity region in the case of high MAI; are described simply by a set of linear constraints.

In addition to the analytical aspects, implementative details of the solution of the two subproblems have been also investigated. Centralized and distributed approaches have been discussed for the network-layer subproblem. Both solutions are iterative and may be selected depending on the application scenario and the network size. The resource-layer has been shown to be efficiently solved by means of an iterative Distributed Resource Allocation Algorithm (DRAA) which entails limited signalling among neighboring nodes and is able to self-adapt to variations in the systems conditions.

Numerical results have shown the potential of the proposed solution. Optimal design problems, which would have otherwise remained unsolved, have been addressed my means of the two-level decomposition. The performance of the MPOP have been tested for unicast, multisession multicast and multi-source scenarios. Comparison with common shortest-path/minimum-cost tree solutions and interference avoiding schemes have been performed. Network coding and source coding gain have been evaluated. Finally, the DRAA convergence, adaptivity and robustness have been investigated.

The two-level decomposition has the appealing property to give insights into a still-unknown solution space of a high complexity optimization problem.

However, it does not suffice to solve *all* instances of such problem. High MAI scenarios may, in fact, lead to loose polyhedral outer bounds and therefore to unsolvable MPOPs. This remains an open problem.

Appendices

A Proof of Proposition 4.3

Under the above reported assumptions about the functions $\Phi(\cdot)$, $J_i(\cdot)$, $\Delta_i(\cdot)$ and $D_i(\cdot)$ present in (3.6.1)-(3.6.10), the resulting MPOP is a convex optimization problem *if and only if* the corresponding multicast capacity region $\mathcal{C}$ in (4.3) is a convex set. Hence, let $\mathcal{C}$ be nonconvex and let $\mathcal{C}_0$ be an assigned convex outer-bound of $\mathcal{C}$. Furthermore, let indicate by

$$(\overrightarrow{f}^*_0, \overrightarrow{x_{10}}^*, \ldots, \overrightarrow{x_{F0}}^*, \mathbf{G}^*_0, \overrightarrow{\Gamma}^*_0, \overrightarrow{P}^*_0, \overrightarrow{C}^*_0), \tag{A.1}$$

the set of parameters obtained by solving the cascade of the $\mathcal{C}_0$-relaxed FNC and the corresponding ERA problems. Thus, proof of Proposition 4.3 relies on the observation that the relaxation induced by the outer bound $\mathcal{C}_0$ leaves *unchanged* both formulation and constraints of the problem in (4.5.1)-(4.5.3). As a consequence, the constraints in (4.5.2)-(4.5.3) of the ERA problem still define the *same* multicast capacity region $\mathcal{C}$ in (4.3) of the MPOP. This consideration allows to state that the ERAP is feasible if and only if the input capacity vector $\overrightarrow{C}^*_0$ obtained by solving the $\mathcal{C}_0$-relaxed FNCP *falls into* the actual $\mathcal{C}$ of (4.3), so that we can write the following basic property:

$$\text{ERAP is feasible} \rightleftarrows \overrightarrow{C}^*_0 \in \mathcal{C} \text{ and } \mathcal{C} \neq \emptyset. \tag{A.2}$$

Now, by leveraging on the above property, we are able to prove the claims of Proposition 4.3. Specifically,

1. let assume the $\mathcal{C}_0$-relaxed FNCP be unfeasible. Thus, since $\mathcal{C}_0$ relaxes $\mathcal{C}$ (i.e., $\mathcal{C}_0 \supseteq \mathcal{C}$) and all constraints in (4.4.2) coincide with those in (3.6.2)-(3.6.10) for the MPOP, we conclude that also the MPOP is *unfeasible*;

2. let assume the $\mathcal{C}_0$-relaxed FNCP be feasible and the resulting ERAP be unfeasible. Thus, due to the property in (A.2), the ERAP is unfeasible when (and only when) *at least one* of the following cases 2.a), 2.b) occurs:

   2.a) $\mathcal{C}$ is empty (i.e., $\mathcal{C}_0 = \emptyset$). This case takes place if and only if the set Π in (4.1) is empty, that is equivalent, in turn, to claim that the MPOP is *unfeasible*;

   2.b) the capacity vector $\overrightarrow{C}_0^*$ in (A.1) is unfeasible for the MPOP (i.e., $\overrightarrow{C}_0^* \notin \mathcal{C}$). Since $\mathcal{C}_0 \supseteq \mathcal{C}$, this case occurs when $\overrightarrow{C}_0^* \in \mathcal{C}_0$ but $\overrightarrow{C}_0^* \notin \mathcal{C}$. This is the case when *no* firm conclusion about the feasibility/unfeasibility of the MPOP can be drawn;

3. let assume both the $\mathcal{C}_0$-relaxed FNCP and the corresponding ERAP be feasible. This means that the resulting capacity-vector $\overrightarrow{C}_0^*$ in (A.1) falls into the MPOP capacity region $\mathcal{C}$ in (4.3), i.e., $\overrightarrow{C}_0^* \in \mathcal{C}$.

   Hence, since the objective function in (4.4.1), all constraints in (4.4.2) *and* (4.5.2)-(4.5.3) of the $\mathcal{C}_0$-relaxed FNC-plus-ERA problem *coincide* with the ones of the MPOP formulation in Section 3.2, we conclude that the solution in (A.1) of the $\mathcal{C}_0$-relaxed FNC-plus-ERA problem *must coincide* with the corresponding solution: $\{\overrightarrow{f}^*, \overrightarrow{x_1}^*, \ldots, \overrightarrow{x_F}^*, \overrightarrow{P}^*, \overrightarrow{\Gamma}^*, \mathbf{G}^*\}$ of the MPOP. This last observation completes the proof of the overall Proposition 4.3.

B Derivation of the per-link session delay in (6.3)

According to the abovementioned Kleinrock's independence assumption and Jackson's Theorem [67], the queueing system of a node may be modelled as an M/M/1 queue with $F \geq 1$ priority classes. Thus, under the (additional) assumption that the implemented service discipline in nonpreemptive, the resulting average queueing-plus-transmission delay $\overline{T}_i(l)$ (s) induced by the l-th link on the i-th conveyed flow can be expressed as [67, eqs(3.82),(3.83)]

$$\overline{T}_i(l) \equiv \frac{1}{C(l)} + \frac{\sum_{m=1}^{F} x_m(l)}{C^2(l)\left[1-\sum_{n=1}^{i-1}\varrho_n(l)\right]\left[1-\sum_{m=1}^{i}\varrho_m(l)\right]} \tag{B.1}$$

where

$$\varrho_m(l) \triangleq x_m(l)/C(l), \quad m = 1, \ldots, F\,, \tag{B.2}$$

is the m-th utilization factor of the l-th link. Therefore, an expansion of the products at the denominator of (B.1) leads to the following chain of inequalities:

$$\begin{aligned}\overline{T}_i(l) &\overset{(a)}{\leq} \frac{1}{C(l)} + \frac{\sum_{m=1}^{F} x_m(l)}{C(l)\left[1-\varrho_i(l)-2\sum_{m=1}^{i-1}\varrho_m(l)\right]} \\ &\overset{(b)}{\leq} \frac{1}{C(l)} + \frac{\eta(l)}{C(l)-x_i(l)-2\sum_{m=1}^{i-1}x_m(l)}\,,\end{aligned} \tag{B.3}$$

where: (a) stems from neglecting all the nonnegative cross-terms: $\varrho_m(l)\varrho_n(l)$, $m \neq n$, embraced by the product at the denominator in (B.1); whereas, (b) arises from a combined exploitation of the defining relationship in (B.2) and the constraint in (3.6.3) on the maximum allowed link utilization. The last expression in (B.3) is that reported in (6.3). It is compliant with all the (general) assumptions listed in Section 3.1 on the considered per-link delay function and approaches actual $\overline{T}_i(l)$ for vanishing link utilization factors.

Bibliography

[1] Y.Chen, T.Farley, N. Ye, "QoS Requirements of Network Applications on the Internet", *Journal of Inf. Knowl. Syst. Manag*, vol.4, no.1, pp.55-76, Jan. 2004.

[2] R.Braden, D.Clark, S.Shenker, "Integrated Services in the Internet Architecture: An Overview", IETF RFC 1633, 1994.

[3] S.Blake, D.Black, M.Carlson, E.Davies, Zh.Wang, W.Weiss, "An architecture for Differentiated Services", IETF RFC 2475, 1998.

[4] Y.Bernet, et al., "A Framework For Integrated Services Operation Over Diffserv Networks", IETF RFC 2998, 2000.

[5] E.Rosen, A.Viswanathan, R.Callon,"Multiprotocol Label Switching Architecture", IETF RFC 3031, 2001.

[6] D.Awduche et al., "Overview and Principles of Internet Traffic Engineering", IETF RFC 3272, 2002.

[7] D. Awduche et al., "MPLS and Traffic Engineering in IP Networks," IEEE *Commun. Mag.*, vol.37, no.12, pp.42-47, Dec. 1999.

[8] B. Fortz et al., "Internet Traffic Engineering by Optimising OSPF Weights," Proc. *IEEE INFOCOM 2000*, pp.519-28, 2000.

[9] B. Fortz, J. Rexford, M.Thorup, "Traffic Engineering with Traditional IP Routing Protocols," *IEEE Commun. Mag.*, vol.40, no.10, pp.118-24, Oct. 2002.

[10] Y. Wang et al., "Internet Traffic Engineering without Full Mesh Overlaying," Proc. *IEEE INFOCOM 2001*, pp.565-71, 2001.

[11] N.Wang, K.Ho, G.Pavlou, M.Howarth, "An overview of routing optimization for internet traffic engineering", *IEEE Communications Surveys & Tutorials*, vol.10, no.1, pp.36-56, Apr. 2008.

[12] A.Sridharam, R.Guerin, C.Diot "Achieving near optimal traffic engineering solutions for current OSPF/IS-IS networks", Proc. *IEEE INFOCOM 2003*, pp.1167-1177, Mar. 2003.

[13] B.A.Movsichoff, C.M.Lagoa, H.Che, "Decentralized Optimal Traffic Engineering in connectionless networks", *IEEE J.Sel.Areas in Communication*, vol.23, pp.293-303, Feb. 2005.

[14] C.E.Perkins, P.Bhagwat, "Highly dynamic Destination-Sequenced Distance-Vector (DSDV) routing for mobile computers", Proc. *ACM SIGCOMM'94*, pp.234-244, Aug. 1994.

[15] D.Johnson, D.Maltz, "Dynamic source routing in ad hoc wireless networks", *Mobile Computing*, Kluwer Academic Publishers, 1996.

[16] C.E.Perkins, E.M.Royer, "Ad hoc on-demand distance vector routing", Proc. *IEEE Workshop on Mobile Computing Systems and Applications*, pp. 90-100, Feb. 1999.

[17] R.Draves, J.Padhye, B.Zile, "Comparisons of Routing Metrics for Static Multi-hop Wireless Networks", Proc. *ACM SIGCOMM'04*, pp.133-144, Sept. 2004.

[18] J.Guerin, M.Portmann, A.Pirzada, "Routing metrics for multi-radio wireless mesh networks", *Telecommunication Networks and Applications Conference 2007*, ATNAC 2007, pp. 343-348, Dec. 2007.

[19] F.Foukalas, V.Gazis, N.Alonistioti, "Cross-layer design proposals for wireless mobile networks: a survey and taxonomy", *IEEE Commun. Surveys Tutorials*, vol.10, no.1, pp.70-85, 2008.

[20] I.F.Akyldiz, X.Wang, W.Wang, "Wireless Mesh Networks: a survey", *Comp. Networks*, no.47, pp.445-487, 2005.

[21] Y.Wu, M.Chiang, S.Y.Kung, "Distributed Utility Maximization for Network Coding Based Multicasting: A Critical Cut Approach", Proc. *Workshop on Network Coding, Theory, & Applications (NetCod)*, 2006.

[22] Y.Xuan, C.T.Lea, "Network-Coding Multicast Networks With QoS Guarantees", *IEEE/ACM Tr. on Networking*, vol.19, no.1, pp.265-274, Feb. 2011.

[23] L.Clien, T.Ho, S.H.Low, M.Chiang, J.C.Doyle, "Optimization Based Rate Control for Multicast with Network Coding", Proc. *IEEE INFOCOM 2007*, pp.1163-1171, May 2007.

[24] Z.Li, B.Li, "Efficient and distributed computation of maximum multicast rates," Proc. *IEEE INFOCOM 2005*, vol.3, Mar. 2005.

[25] D.S.Lun, N.Ratnakar, R.Koetter, M.Medard, E.Ahmed, L.Hyunjoo, "Achieving minimum-cost multicast: a decentralized approach based on network coding," Proc. *IEEE INFOCOM 2005*, vol.3, pp.1607-1617, Mar. 2005.

[26] T.Ho, D.S.Lun, *Network Coding - An Introduction*, Cambridge Press, 2008.

[27] R.Ahlswede, N.Cai, S.Y.R.Li, R.W.Yeung, "Network information flow," *IEEE Tr. on Information Theory*, vol.46, no.4, pp.1204-1216, Jul. 2000.

[28] P.A.Chou, Y.Wu, K.Jain, "Practical network coding", *Annual Allerton Conference on Communication, Control, and Computing*, Oct. 2003.

[29] J.E.Wieselthier, G.D.Nguyen, A.Ephremides, "On the Construction of Energy-Efficient Broadcast and Multicast Trees in Wireless Networks", in *Proc. IEEE Computer and Communications*, pp 586-594, Tel Aviv, Israel, 2000.

[30] D.S.Lun, N.Ratnakar, R.Koetter, M.Medard, E.Ahmed, L.Hyunjoo, "Minimum-cost multicast over coded packet networks", *IEEE Tr. on Information Theory*, vol.52, no.6, pp.2608-2623, Jun. 2006.

[31] Y.Wu, P.A.Chou, Q.Zhang, K.Jain, W.Zhu, S.Y.Kung, "Network Planning in Wireless ad-hoc Networks: A Cross-Layer Approach", *IEEE Jr. on Selected Areas in Communication*, vol.23, no.1, pp.136-150, Jan. 2005.

[32] Y.Wu, P.A.Chou, S.Y.Kung, "Minimum-Energy Multicast in Mobile ad-hoc Networks using Network Coding", *IEEE Tr. on Communications*, vol.53, no.11, pp.1906-1918, Nov. 2005.

[33] L.Xiao, M.Johansson, S.Boyd, "Simultaneous routing and resource allocation via dual decomposition," *IEEE Tr. on Communications*, vol.52, no.7, pp.1136-1144, Jul. 2004.

[34] X.Wang, "Fair Energy-Efficient Network Design for Multihop Communications," Proc. *IEEE Sensor Mesh and Ad Hoc Communications and Networks (SECON)*, pp.1-9, 21-25 Jun. 2010.

[35] M.Johansson, L.Xiao, "Cross-layer optimization of wireless networks using nonlinear column generation," *IEEE Tr. on Wireless Communications*, vol.5, no.2, pp.435- 445, Feb. 2006.

[36] L.Chen, S.H.Low, M.Chiang, J.C.Doyle, "Cross-Layer Congestion Control, Routing and Scheduling Design in Ad Hoc Wireless Networks," Proc. *IEEE INFOCOM 2006*, pp.1-13, Apr. 2006.

[37] X.Wang, G.B.Giannakis, "Power-Efficient Resource Allocation for Time-Division Multiple Access Over Fading Channels," *IEEE Tr. on Information Theory*, vol.54, no.3, pp.1225-1240, Mar. 2008.

[38] K.Jain, J.Padhye, V.Padmanabhan, L.Qiu, "Impact of interference on multi-hop wireless network performance," in Proc. *ACM MobiCom*, pp. 66-80, 2003.

[39] D.Traskov, M.Heindlmaier, M.Medard, R.Koetter, D.S.Lun, "Scheduling for Network Coded Multicast: A Conflict Graph Formulation", Proc. *IEEE GLOBECOM Workshops 2008*, pp.1-5, Dec. 2008.

[40] S.Hayashi, Z.Q.Luo, "Spectrum Management for Interference-Limited Multiuser Communication Systems," *IEEE Tr. on Information Theory*, vol.55, no.3, pp.1153-1175, Mar. 2009.

[41] R.Bhatia, M.Kodialam, "On power efficient communication over multi-hop wireless networks: joint routing, scheduling and power control," Proc. *IEEE INFOCOM 2004*, vol.2, pp.1457-1466 vol.2, 7-11 Mar. 2004.

[42] T.Cui, L.Chen, T.Ho, "On Distributed Scheduling in Wireless Networks Exploiting Broadcast and Network Coding", *IEEE Tr. on Communications*, vol.58, no.4, pp.1223-1234, Apr. 2010.

[43] R.L.Cruz, A.V.Santhanam, "Optimal routing, link scheduling and power control in multihop wireless networks," Proc. *IEEE INFOCOM 2003*, pp. 702-711, Apr. 2003.

[44] P.Moberg, "Simultaneous Routing and Resource Allocation in Multihop Wireless Networks using Optimization", Proc. *IEEE GLOBECOM 2006*, pp. 1-5, Dec. 2006.

[45] J.Huang, R.A.Berry, M.L.Honig, "Distributed interference compensation for wireless networks", *IEEE Jr. on Selected Areas in Communication*, vol.24, no.5, pp.1074-1084, May 2006.

[46] M.Chiang, C.W.Tan, D.P.Palomar, D.O'Neill, D.Julian, "Power Control By Geometric Programming," *IEEE Tr. on Wireless Communications*, vol.6, no.7, pp.2640-2651, Jul. 2007.

[47] Y.Nesterov, A.Nemirovsky, *Interior Point Polynomial Methods in Convex Programming*, SIAM Press, 1994.

[48] Y.Xi, E.M.Yeh, "Node-Based Optimal Power Control, Routing and Congestion Control in Wireless Networks," *IEEE Tr. on Information Theory*, vol.54, no.9, pp.4081-4106, Sept. 2008.

[49] Y.Xi, E.M.Yeh, "Distributed Algorithms for Minimum Cost Multicast With Network Coding", *IEEE/ACM Tr. on Networking*, vol.18, no.2, pp.379-392, Apr. 2010.

[50] C.W.Tan, D.Palomar, M.Chiang, "Exploiting hidden convexity for flexible and robust resource allocation in cellular networks", Proc. *IEEE INFOCOM 2007*, pp.964-972, May 2007.

[51] H.Boche, S.Stanczak, "Log-convexity of the minimum total power in CDMA systems with certain quality-of-service guaranteed," *IEEE Tr. on Information Theory*, vol.51, no.1, pp.374-381, Jan. 2005.

[52] H.Boche, S.Stanczak, "On the convexity of feasible QoS regions," *IEEE Tr. on Information Theory*, vol.53, no.2, pp.779-783, Feb. 2007.

[53] J.Yuan, Z.Li, W.Yu, B.Li, "A Cross-Layer Optimization Framework for Multihop Multicast in Wireless Mesh Networks", *IEEE Jr. on Selected Areas in Communication*, vol.24, no.11, pp.2092-2103, Nov. 2006.

[54] K.Rajawat, N.Gatsis, G.B.Giannakis, "Cross-Layer Designs in Coded Wireless Fading Networks With Multicast," *IEEE/ACM Tr.on Networking*, vol.19, no.5, pp.1276-1289, Oct. 2011.

[55] T.Ho, M.Medard, R.Koetter, D.R.Karger, M.Effros, J.Shi, B.Leong, "A random linear network coding approach to multicast", *IEEE Tr. on Information Theory*, vol.52, no.10, pp.4413-4430, Oct. 2006.

[56] D.Slepian, J.W.Wolf, "Noiseless coding of correlated information sources", *IEEE Tr. on Information Theory*, vol.19, no.4, pp.471-480, Jul. 1973.

[57] A.Ramamoorthy, K.Jain, P.A.Chou, M.Effros, "Separating distributed source coding from network coding", *IEEE Tr. on Information Theory*, vol.52, no.6, pp.2785-2795, June 2006.

[58] V.Stankovic, A.D.Liveris, Z.Xiong, C.N.Georghiades, "On code design for the Slepian-Wolf problem and lossless multiterminal networks", *IEEE Tr. on Information Theory*, vol.52, no. 4, pp.1495-1507, Apr.2006.

[59] Y.Wu, V.Stankovic, Z.Xiong, S.Y.Kung, "On practical design for joint distributed source and network coding", *IEEE Tr. on Information Theory*, vol.55, no.4, pp.1709-1719, Apr. 2009.

[60] R.Cristescu, B.B.Lozano, M.Vetterli, "Networked Slepian-Wolf: Theory, Algorithms, and Scaling Laws", *IEEE Tr. on Information Theory*, vol.51, no.12, pp.4057-4073, Dec. 2005.

[61] T.Cui, T.Ho, L.Chen, "Distributed minimum cost multicasting with lossless source coding and network coding", *Proc.of 46th IEEE Conf. on Dec. and Contr.*, New Orleans(USA), pp.506-511, Dec. 2007.

[62] A.Ramamoorthy, "Minimum cost distributed Source coding over a Network", *IEEE Tr. on Information Theory,* vol.57, no.1., pp.461-475, Jan. 2011.

[63] A.Roumy, D.Gesbert, "Optimal matching in wireless sensor networks", *IEEE Proc. of ISIT'07*, pp.2116-2120, 2007.

[64] S.Li, A.Ramamoorthy, "Rate and power allocation under the pairwise distributed source coding constraint", *IEEE Tr. on Communication*, vol.57, no.12, pp.3771-3781, Dec. 2009.

[65] M.Chiang, S.H.Low, A.R.Calderbank, J.C.Doyle, "Layering as Optimization Decomposition: A Mathematical Theory of Network Architectures," *Proceedings of the IEEE*, vol.95, no.1, pp.255-312, Jan. 2007.

[66] M.Pioro, D.Medhi, *Routing, flow, and Capacity design in Communication and Computer Networks*, Elsevier, 2004.

[67] D.P.Bertsekas, R.Gallagher, *Data Networks*, Second Ed., Englewood Cliffs, NJ, Prentice Hall, 1992.

[68] A.Eryilmaz, D.S.Lun, "Control for Inter-session Network Coding", Proc. *Workshop on Network Coding, Theory, & Applications (NetCod)*, San Diego, Jan. 2007.

[69] Z.Li, B.Li, D.Jiang, L.C.Lau, "On achieving optimal throughput with network coding," Proc. *IEEE INFOCOM 2005*, vol.3, pp.2184-2194, Mar. 2005.

[70] D.Tse, P.Viswanath, *Fundamentals of Wireless Communication*, Cambridge University Press, 2004.

[71] X.Qiu, K.Chawla, "On the performance of adaptive modulation in cellular systems," *IEEE Tr. on Communications*, vol.47, no.6, pp.884-895, Jun. 1999.

[72] J.Yan, K.Katrinis, M.May, B.Plattner, "Media and TCP-friendly Congestion Control for scalable video streams", *IEEE Tr. on Multimedia*, vol.8, no.2, pp.196-206, Apr. 2006.

[73] S.Bhadra, S.Shakkottai, P.Gupta, "Min-Cost Selfish Multicast With Network Coding," *IEEE Tr. on Information Theory*, vol.52, no.11, pp.5077-5087, Nov. 2006.

[74] J.He, M.Bresler, M.Chiang, J.Rexford, "Towards Robust Multi-Layer Traffic Engineering: Optimization of Congestion Control and Routing", *IEEE J.Sel.Areas in Communication*, vol.25, no.5, pp.868-880, Jun. 2007.

[75] T.Rougharden, E.Tardos, "How Bad is Selfish Routing?", *Journal of ACM*, vol.49, no.2, pp.236-259, Mar. 2002.

[76] M.V.d.Schaar, P.A.Chou, *Multimedia over IP and Wireless Networks*, Academic Press, 2007.

[77] S.S.Pradhan, K.Ramchandran, "Distributed source coding using syndromes (DISCUS): design, and construction", *IEEE Tr. on Information Theory*, vol.49, no.3, pp.626-643, Mar. 2003.

[78] P.L.Dragotti, M.Gatspar, *Distributed Source Coding - Theory, Algorithms and Applications*, Elsevier, 2009.

[79] M.S.Bazaraa, D.Sherali, C.M.Shetty, *Nonlinear Programming: Theory and Algorithms*, Wiley, 3rd Ed., 2006.

[80] H.J.Kushner, G.G.Yin, *Stochastic Approximation Algorithm and Application*, Springer, 2nd Ed., 2003.

[81] H.J.Kushner, J.Yang, "Analysis of adaptive stepsize SA algorithms for parameter tracking", *IEEE Tr. on Automatic Control*, vol.40, no. 8, pp 1403-1410, Aug. 1995.

[82] J.Zhang, D.Zheng, M.Chiang, "The Impact of Stochastic Noisy Feedback on Distributed Network Utility Maximization," *IEEE Tr. on Information Theory*, vol.54, no.2, pp.645-665, Feb. 2008.

[83] A.Michail, A.Ephremides, "Algorithms for routing session traffic in wireless ad-hoc networks with energy and bandwidth limitations", *Proc.of 12th IEEE Int.Symp. on Per.,Ind.,and Mob. Radio Comm.*, 2001.

[84] S.Deering, D.Estrin et al., "The PIM architecture for Wide area multicasting", *IEEE/ACM Tr. on Networking*, vol.4,no.2, pp.153-162, Apr. 1996.

[85] E.Baccarelli, N.Cordeschi, V.Polli, "Jointly Optimal Congestion Control, Network Coding and Power Control for QoS Multicast over DiffServ MAI-affected Wireless Networks", *International Conference on Wireless Networks*, Las Vegas, Jul. 2011.

[86] N.Cordeschi, V.Polli, E.Baccarelli, "Traffic Engineering for wireless connectionless access networks supporting QoS-demanding media applications", *Computer Networks*, Elsevier, Sept. 2011.

[87] E.Baccarelli, N.Cordeschi, V.Polli, "QoS Traffic Engineering for self-adaptive Resource Allocation in MAI-affected Wireless Networks", *IEEE GLOBECOM 2011*, Houston, US, Dec. 2011.